IEEE Access
Multidisciplinary | Rapid Review | Open Access Journal

Received August 9, 2020, accepted August 24, 2020, date of publication September 4, 2020, date of current version September 23, 2020.

Digital Object Identifier 10.1109/ACCESS.2020.3021754

Fuel Cell Parameters Estimation via Marine Predators and Political Optimizers

AHMED A. ZAKI DIAB[1], MOHAMED A. TOLBA[2,3], (Member, IEEE), AYAT GAMAL ABO EL-MAGD[4], MAGDY M. ZAKY[5], AND ALI M. EL-RIFAIE[6], (Senior Member, IEEE)

[1]Electrical Engineering Department, Faculty of Engineering, Minia University, Minia 61111, Egypt
[2]Nuclear Research Center, Reactors Engineering Department, Egypt Second Research Reactor-2, Egyptian Atomic Energy Authority, Cairo 11787, Egypt
[3]Electrical Power System Department, Moscow Power Engineering Institute, 111250 Moscow, Russia
[4]Electrical and Computer Department, El-Minia High Institute of Engineering and Technology, Minia 61519, Egypt
[5]Nuclear Research Center, Engineering Department, Egypt Second Research Reactor-2, Egyptian Atomic Energy Authority (EAEA), Cairo 11787, Egypt
[6]College of Engineering and Technology, American University of the Middle East, Kuwait City 15453, Kuwait

Corresponding authors: Ahmed A. Zaki Diab (a.diab@mu.edu.eg), Mohamed A. Tolba (matolba@ieee.org), and Ali M. El-Rifaie (ali.el-rifaie@aum.edu.kw)

ABSTRACT Proton Exchange Membrane Fuel Cells (PEMFC) is considered a propitious solution for an environmentally friendly energy source. A precise model of PEMFC for accurate identification of its polarization curve and an in-depth understanding of all its operating characteristics attracted the interest of many researchers. In this paper, recent meta-heuristic optimization methods have been successfully applied to evaluate the unknown parameters of PEMFC models, particularly Marine Predators Algorithm (MPA) and Political Optimizer (PO) techniques. The proposed optimization algorithms have been tested on three different commercial PEMFC stacks, namely BCS 500-W, SR-12PEM 500 W, and 250 W stack under various operating conditions. The sum of square errors (SSE) between the results obtained by the application of the estimated parameters and the experimentally measured results of the fuel cell stacks was considered as the objective function of the optimization problem. In order to validate the effectiveness of the proposed methods, the results are compared with those obtained in the literature. Moreover, the I/V curves obtained by the application of MPA and PO showed a clear matching with datasheet curves for all the studied cases. Statistical analysis has been performed to evaluate the robustness of the MPA and PO techniques. Finally, the PEMFC model based on the MPA technique surpasses all compared algorithms in terms of the solution accuracy and the convergence speed. The obtained results confirmed the superiority and reliability of the applied approach of the MPA algorithm. The results prove that the MPA algorithm has a superior performance based on its reliability.

INDEX TERMS Fuel cell modeling, parameter estimation, metaheuristic algorithms.

I. INTRODUCTION

The greenhouse gases and the depletion of fossil fuels have provoked the governments and industries to invest more in renewable energy sources (RES) such as PV, Wind, Tidal, Wave ...etc. Utilizing such new RES into power grids takes new trends. It can be harnessed as a smart micro-grid or can be integrated as an isolated standalone AC-DC power grid [1]. However, due to its stochastic nature and during load peak-hours, back-up supports are needed. Fuel cells are an elegant choice that can play an important role in such upcoming power grids.

A reliable on-site emergency power supply is one of the most important systems used to assure the safety of nuclear reactors, which fulfills the safe shutdown, remove the heat after shutdown and plant confinement. In the case of Loss of Off-site Power Supply (LOPS) or plant blackout the reliable on-site emergency plays the main role in safe the plant and to protect the public and environment against radiation hazards as a consequence of LOPS. At the current situation, most of the nuclear reactors utilize independent diesel generator sets as on-site emergency power supply to act as a reliable electric source to guarantee the safety functions of the plant [2]. In the last decade the green energy resources became attractive to minimize the global warming and protect the environment from the effect of the burned of fossil fuel, that produced

The associate editor coordinating the review of this manuscript and approving it for publication was Lei Wang.

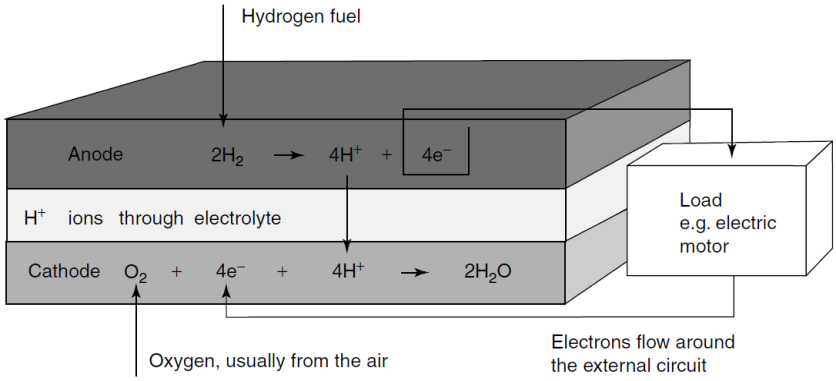

FIGURE 1. **Electrode reactions and flow of charge in fuel cell.**

CO2 [3], [4]. Fuel cells system can be used to improve the backup power system performance in nuclear reactors. This will feed the reactor the emergency cooling system in cases of LOPS, Loss of Flow Accident and Loss of Coolant Accident (LOCA) and continue cooling the reactor core to prevent the core melting down and mitigate the consequences as a part of the defense in depth philosophy [2], [3].

Fuel cells can be categorized into numerous types such as Proton-Exchange Membrane Fuel Cells, from Perfluorosulfonic Acid (PFSA) to Hydrocarbon Ionomers, Direct Hydrocarbon Solid Oxide Fuel Cells, Solid Oxide Fuel Cells, Polybenzimidazole Fuel Cells, etc. [3]. On the other hand, there is a great work has been done in the last decade to use the hydrogen fuel cells in nuclear sites because nuclear energy can be used as the primary energy source for hydrogen production. Moreover, it is attractive because of the greenhouse gas emissions associated with nuclear energy production are much lower than those with conventional fossil fuel combustion. Nuclear energy is adaptable to large-scale hydrogen production [2]. Generally using fuel cells as a part of the electrical resources in the design, operation, and maintenance of nuclear power plants will enhance the reliability of on-site emergency power sources and save the plant against LOPS and plant blackout accidents.

Since 1990, fuel cell development has progressed rapidly. Car manufactures, and heating firms have discovered the technology and aim to benefit from its positive image. Fuel cell operation is based on the chemical reaction that occurs under controlled conditions. A Fuel cell consists of an electrode and a cathode with an electrolyte between them. The anode is fed by pure hydrogen (H2) or a flamed gas containing hydrogen, while oxygen (O2) or air is fed to the cathode. Depending on electrolyte, gases used as a fuel and the operating temperature, there are various classifications for the fuel cells. The polymer electrolyte fuel cell (PEFC) and proton exchange membrane fuel cell (PEMFC) are the most commonly used types. Its operating temperature is around 800C, and it can run on with normal air and reformed hydrogen as a fuel [5].

The mathematical model of the fuel cell is considered as the milestone on which the designing and testing of the fuel cell can be performed in an appropriate way. Moreover, a good mathematical model is essential to move forward the integration of the fuel cell besides supporting the designers with more information about the physical phenomena occurring inside it. The electrochemical model of the fuel cell has essential empirical and semi-empirical equations that depend on a combination set of unknown parameters. The inherited coupled parameters make the modeling of a fuel cell more difficult, which motivates the researcher to search for a suitable solution. Due to its sufficient way to obtain optimum solutions for complicated problems, Meta-heuristics can be adapted to provide robust parameter estimation for fuel cell modeling. From this fact, the no-free-lunch theorem has made a cogent remark that is employed by several optimization techniques to solve various engineering optimization problems [6], [7].

The adaptive differential evolution algorithm (ADE) is one of the competitive methods which have been used for solving the parameter estimation for PEMFC [8]. The main contribution of the proposed ADE method is to decrease premature convergence and increase search efficiency. Hybrid adaptive differential evolution is introduced in [9]. It is a combination set between biological genetic strategy and bee colony foraging method. The first method enhances the parametric scaling for dynamic cross-over probability, while the former method improves the weak local search. Hence, the ADE enhances the performance of the optimization techniques. A grouping-based global harmony search algorithm (GGHS) has been adopted for obtaining a precise estimation for PEMFC parameters, as reported in [10]. The algorithm performance was compared with different methods such as particle swarm optimization (PSO) and seeker optimization algorithm (SOA). From the comparison, it had been concluded that the GGHS platform exhibits better performance than other algorithms [10]. The genetic algorithm has been applied for parameter estimation of PEMFC [11]–[13]. In [11], a new formulation based on a genetic algorithm

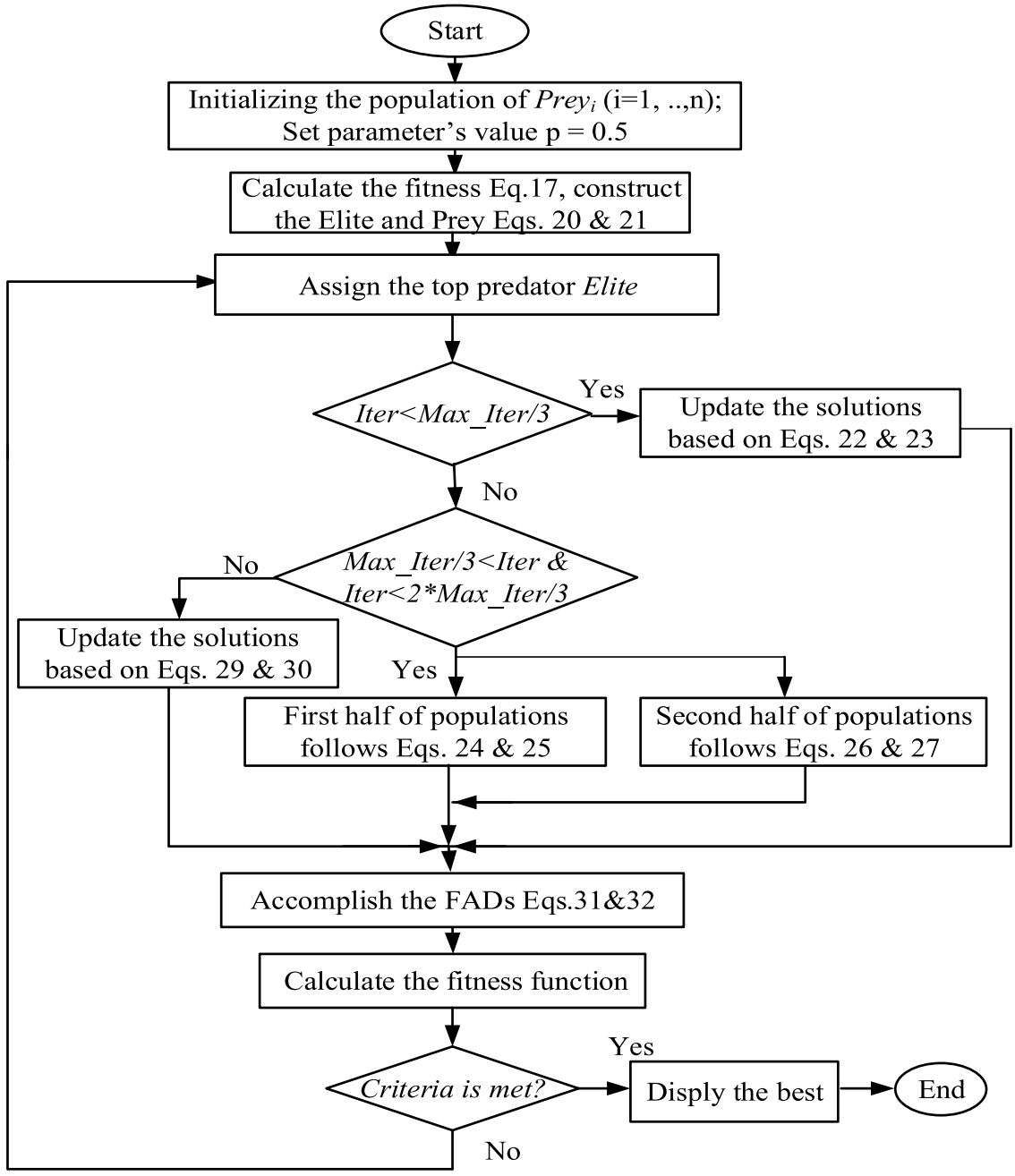

FIGURE 2. Flowchart of MPA optimization technique.

(GA) is used to deal with fuel cell parameter evaluation. The main advantage of this method is lower complexity, less time consumption, enhancing accuracy and ease of implementation. A hybrid combination set between teaching learning-based optimization method (TLBO) and Differential Evaluation Algorithm (DE) is introduced in [14] to obtain a proper estimation for the parameter model of PEMFC. The (TLBO-DE) performance is compared with different optimization algorithms. The TLBO-DE proves its accuracy and robustness, besides its ability to obtain an optimum solution with lesser computation time. The Grey Wolfe Optimization (GWO) algorithm is used for identifying the PEMFC model parameters [15]. An experimental test is performed to prove a superior performance for GWO to other optimization methods such as Antlion Optimizer (ALO), and Dragonfly Algorithm (DA). New meta-heuristic approaches have been employed to adapt the PEMFC model parameter such as Grasshopper Optimization Algorithm (GOH), Slap Swarm Optimizer (SSO) and Shark Smell Optimizer (SSO) [16]–[18]. The advantages of these methods are better

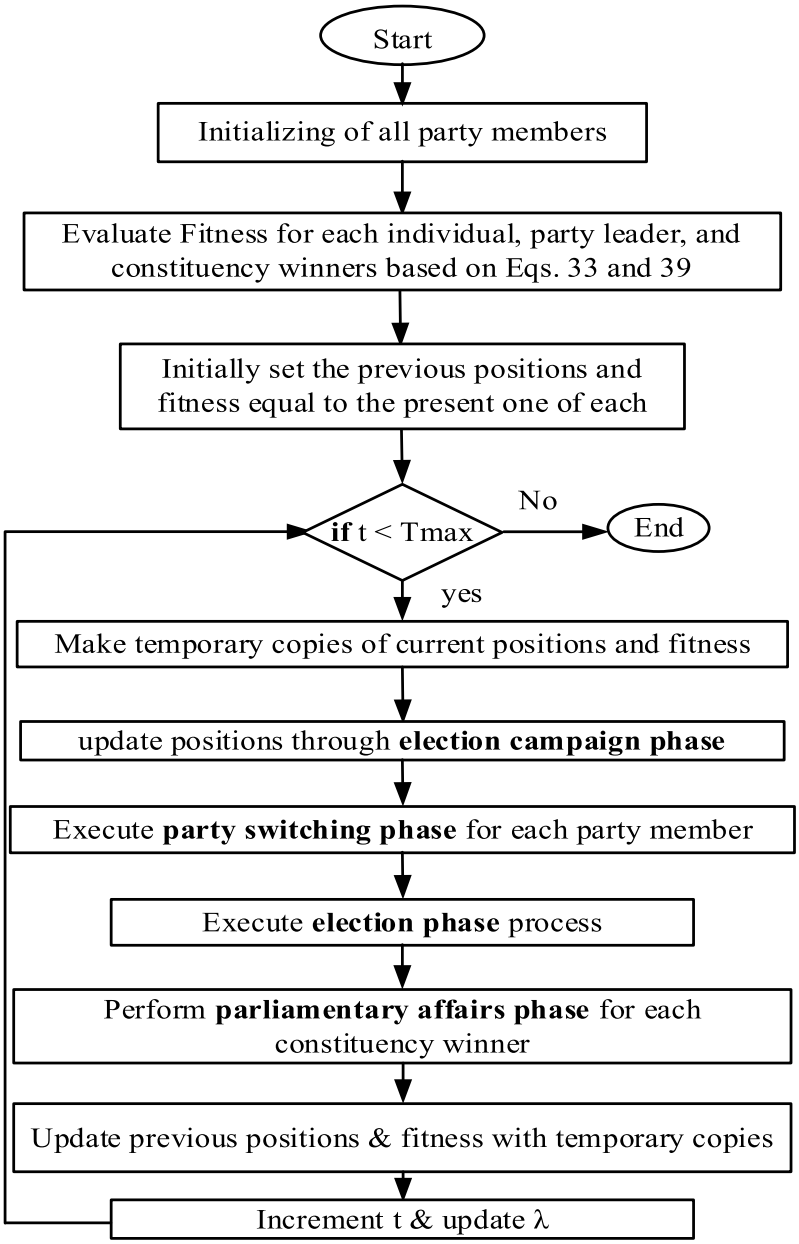

FIGURE 3. Flowchart of PO optimization technique.

convergence to an optimum solution, tuning its controlling parameters with the low effort of computation, and faster process execution. In [19], JAYA algorithm was deployed to estimate the PEMFC parameters effectively. Compared to other optimization techniques, JAYA has better convergence time, accuracy, and stability. In [20], the Cuckoo Search (CS) algorithm is used to obtain the parameters of the PEMFC. The author has proposed an explosion operator to fine-tune the step size of the CS. The Cuckoo Search Algorithm with Explosion Operator (CS-EO) proves its ability to avoid precipitate convergence and enhances the overall performance of the CS. According to [21], the hybrid optimizer based on the vortex search algorithm (VSA) and differential evolution (DE) has been developed to evaluate the optimum uncertain parameters of the PEMFC. Both VSA and DE had been incorporated to increase the attitude of VSA preventing its local-optima by promoting the operating of exploitation followed in VSA based on DE. From [22], it has been applied prepared and utilized the Modified Artificial Ecosystem Optimization (MAEO) to estimate the parameters of PEMFC. In this technique, the MAEO was very effective to increase the attitude of AEO for introducing a very fast process of convergence to avoid the local optima. In [23], the authors proposed and utilized the Hybrid Grey Wolf

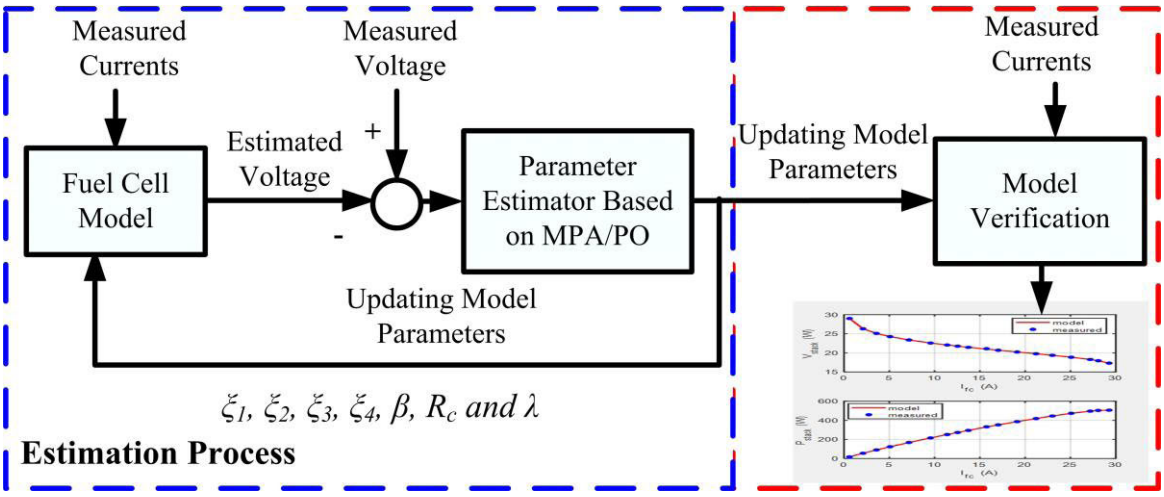

FIGURE 4. Global parameter estimation representation.

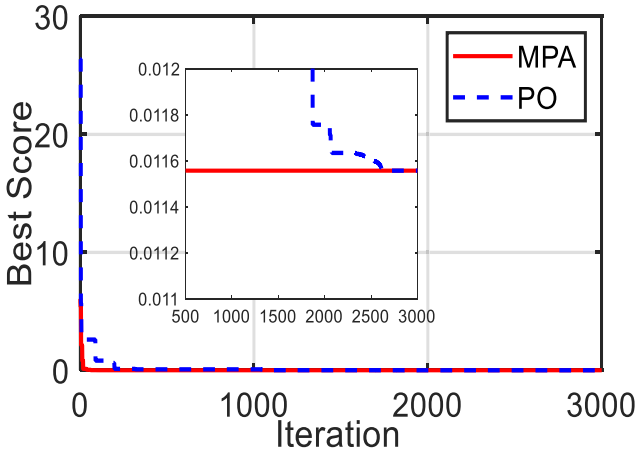

FIGURE 5. Convergence curve of MPA and PO optimization algorithms.

Optimizer (HGWO) to solve the problems of the parameters extraction of PEMFC. The HGWO has been used to combine the ≪crossover and mutation operators≫ during the optimization evaluation to enhance the ability of the search potential avoiding the trapping in local-optima. Moreover, Harris Hawks Optimization (HHO) algorithm has been applied for extracting the parameters of the PEMFC model in Refs. [31]–[34]. The obtained results in the reported references [31]–[34] prove the ability of the HHO to estimate the parameters of PEMFC. A comparison between the reported results from references [31]–[34] and those of the MPA and PO algorithms will be presented in the results section to evaluate the effectiveness of each algorithm. All these algorithms are presented and applied for estimating the parameters of the PEMFC Model for improving the estimation accuracy. However, most of these works could not strengthen the estimation accuracy. Therefore, it is necessary to present and validate recent methods that have the ability to accurately estimate the parameters of the PEMFC Model with good convergence characteristics.

Recently one of the outstanding optimization techniques that have been discovered not a long time ago is the MPA [24]. It has a superior performance to act with global optimization problems rather than the other optimization techniques. It possesses a better exploration of the optimum solution without getting stacked to the local search. Moreover, a contemporary optimization method has been proposed to solve complicated problems; this method is the PO method [25]. It is a simple structure method. Its advantages underlying, fewer controlling parameters, self-adaption to its parameters, can be adapted easily with other methods to obtain better convergence for optimal solutions. However, this method is not deeply applied to solve electrical engineering problems.

In this paper, MPA and PO have been used for estimating the parameters of a number of commercial proton exchange membrane fuel cells. To validate the effectiveness of the MPA and PO methods, comparisons and different operating scenarios have been studied. The contribution of this work includes the implementation of two unprecedented optimization algorithms, namely MPA and PO, for defining the equivocal parameters of the fuel cell model and comprehensive comparison with other competitive techniques that have been provided in the literature.

II. PROBLEM FORMULATION

A. BASIC PHYSICAL OPERATION

Fuel cells are considered a direct method of converting chemical energy into electrical energy. The construction of a typical proton exchange membrane (PEM) fuel cell is described in Fig. 1. As seen from the figure, the PEM fuel cell model comprises two electrodes (anode and cathode), between which a catalyst and membrane layers are stacked. In addition, at the anode and cathode sides, two channels are used for supplying hydrogen and air, which will be diffused through the electrodes.

A simple way of understanding the base operation of the fuel cell is to say that the hydrogen gas is being 'burnt'

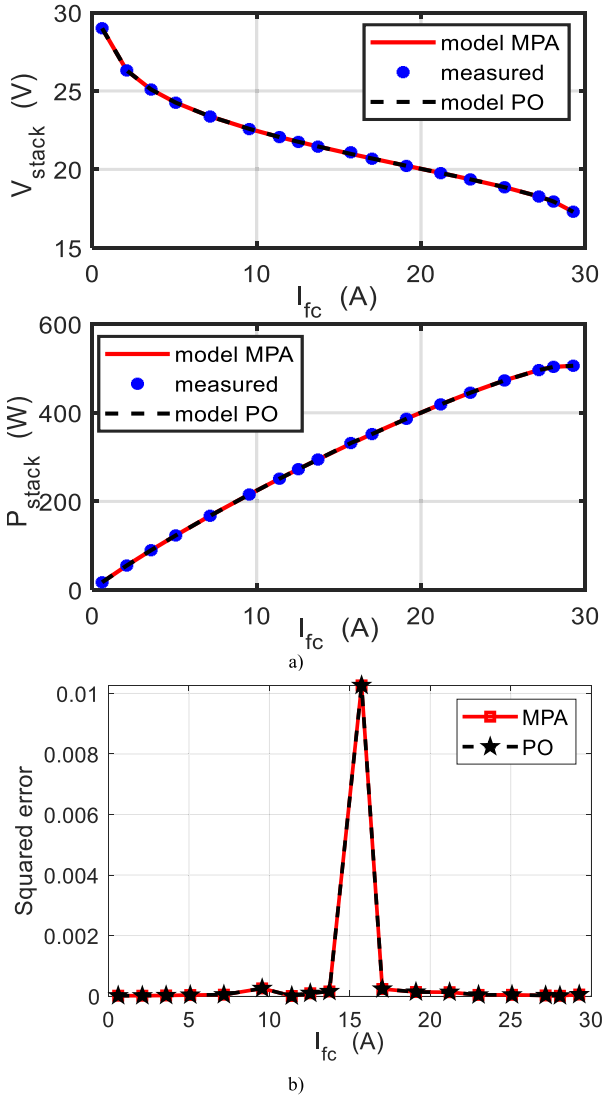

FIGURE 6. a) The I/V and I/P curve characteristics and b) Squared error between the estimated and measured data of BCS 500W based on MPA and PO optimization algorithms.

or combusted in the simple chemical reaction described as follows [26]:

$$2H_2 + O_2 \rightarrow 2H_2O \tag{1}$$

However, in this case, instead of heat energy being released, electrical energy is generated. The reaction takes place at the anode and cathode and can be declared as follows:

$$2H_2 \rightarrow 4H^+ + 4e^- \tag{2}$$

At the anode of the fuel cell, the hydrogen gas ionizes, releasing electrons and creating H^+ ions (or protons).

This reaction releases electrical energy presented by the negative electrons e^-. At the cathode side, oxygen reacts with the electrons which are taken from the injected air at the electrode and the H^+ ions produced from the electrolyte, to finally form water, and it can be expressed as:

$$O_2 + 4e^- \rightarrow 2H_2O \tag{3}$$

B. MATHEMATICAL MODEL OF PEMFC

An electrochemical-based model for PEMFC has been adopted by Amphlett *et al.* [27], which considered a number of fuel cells N cells connected in series to form a fuel cell stack system. This model is a helpful tool for engineers interested in evaluating the performance of PEMFC and optimizing the system parameters. The output voltage across the terminals of the fuel cell stack can be presented as follows [9]:

$$V_{Fc} = N_{cells} \times (E_{Nernst} - V_{act} - V_{ohmic} - V_{con}) \tag{4}$$

where V_{act} presents the activation voltage drop caused by the kinetics of the chemical reactions around the surface of the electrodes, which causes a sharp drop in the I/V polarization curve of the fuel cell stack at lower currents [12]. V_{ohmic} presents the ohmic voltage drop, which results from the resistance of transferring the protons and electrons in the electrolyte. For intermediate currents, the ohmic voltage drops smoothly and linearly as a result of the ohmic losses. V_{con} is the concentration voltage drop, which appears due to the sophisticated processes of transport, and which lets the output voltage of the fuel cell fall sharply another time at higher currents [28]. The E_{Nernst} represents the fuel cell reversible voltage in an open circuit electrodynamic balance and is calculated using (5) [9]–[11]:

$$E_{Nernst} = 1.229 - 0.85 \times 10^{-3}\,(T - 298.15) + 4.3085 \times 10^{-5} \times T \left[\ln\left(P_{H_2}\right) - \frac{1}{2}\ln\left(P_{O_2}\right)\right] \tag{5}$$

where T is the operating temperature of the fuel cell in Kelvin; P_{H2} and P_{O2} denote for the partial pressures of hydrogen and oxygen, respectively. The partial pressure of the gases depends on the nature of the components of the chemical reaction. If the components of the chemical reaction are air and hydrogen, then according to [15], [29], the partial pressure of each reactant can be estimated by the following formulas:

$$P_{N_2} = \frac{0.79}{0.21} P_{O_2} \tag{6}$$

where:

$$P_{O_2} = P_c - RH_c P^{sat}_{H_2O} - P_{N_2} \times \exp\left(\frac{0.291\left(I_{fc}/A\right)}{T^{0.832}}\right) \tag{7}$$

The saturation pressure of the water vapor P^{sat}_{H2O} is estimated by the following expression:

$$\log_{10}\left(P^{sat}_{H_2O}\right) = 2.95 \times 10^{-2}\,(T - 273.15) - 9.18 \times 10^{-5} \times (T - 273.15)^2 + 1.44 \times 10^{-7}\,(T - 273.15)^3 - 2.18 \tag{8}$$

when the reactants are oxygen and hydrogen, then the formula (8) can be as follows:

$$P_{O_2} = RH_c P^{sat}_{H_2O} \times \left[\left(\exp\left(\frac{4.192\left(I_{fc}/A\right)}{T^{1.334}}\right) \times \frac{RH_c P^{sat}_{H_2O}}{P_a}\right)^{-1} - 1\right] \tag{9}$$

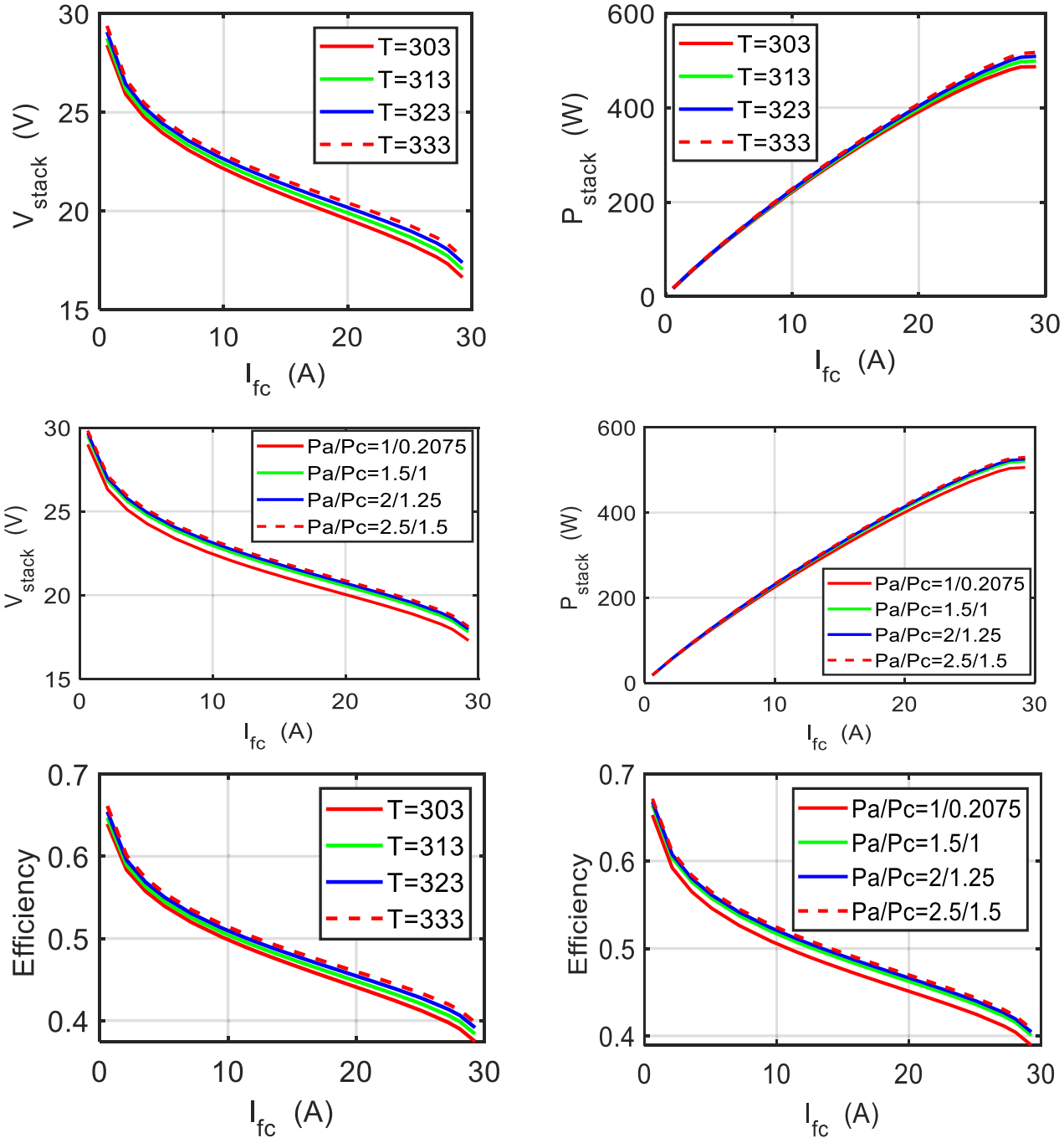

FIGURE 7. Characteristics of BCS 500W with the variation of the Temperature and pressure based on MPA optimization algorithm.

The partial pressure of hydrogen *PH2* in both conditions can be calculated from the following expression:

$$P_{H_2} = 0.5 RH_a P^{sat}_{H_2O} \times \left[\left(\exp\left(\frac{1.635\left(I_{fc}/A\right)}{T^{1.334}} \right) \times \frac{RH_a P^{sat}_{H_2O}}{P_a} \right)^{-1} - 1 \right] \quad (10)$$

where RH_c and RH_a are the relative humidity of vapor at the cathode and anode, respectively. While P_a and P_c are the channel pressure (atm) at the anode and cathode, respectively; P_{N2} is the partial pressure of nitrogen at the flow channel of gas at the cathode (atm) and A is the active surface area of the membrane.

The activation voltage drop V_{act} can be determined as follows [11]:

$$V_{act} = -\left[\xi_1 + \xi_2 T + \xi_3 T \ln\left(C_{O_2}\right) + \xi_4 T \ln\left(I_{fc}\right)\right] \quad (11)$$

where $\xi_1, \xi_2, \xi_3, \xi_4$ present semi-empirical coefficients; I_{fc} is the output current from the fuel cell stack; C_{O2} is the concentration of oxygen at the surface of the cathode (mol.cm^{-3})

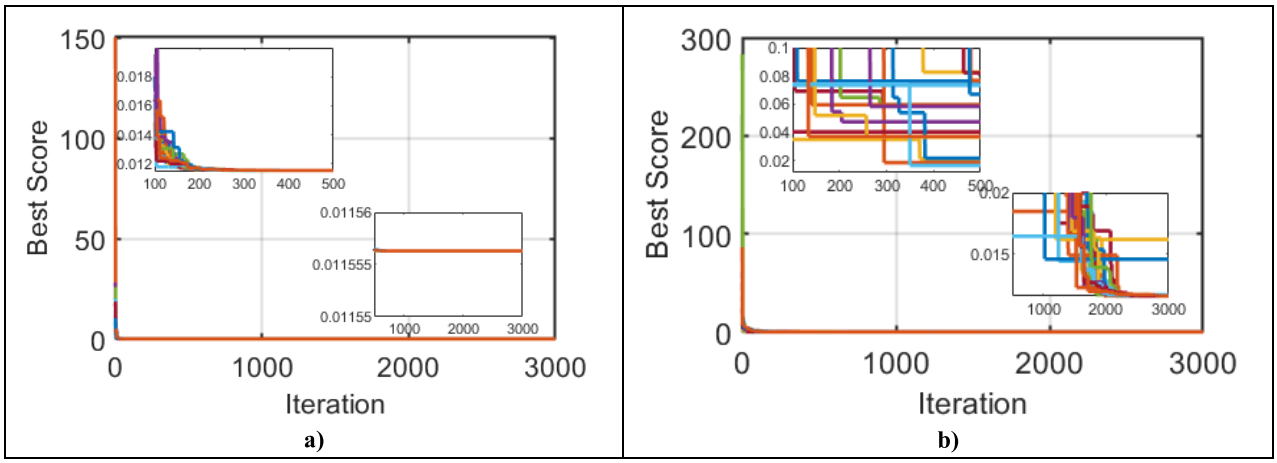

FIGURE 8. Convergence trends of the fitness function over the 30 runs for application a) MPA and b) PO with the case of BCS 500W.

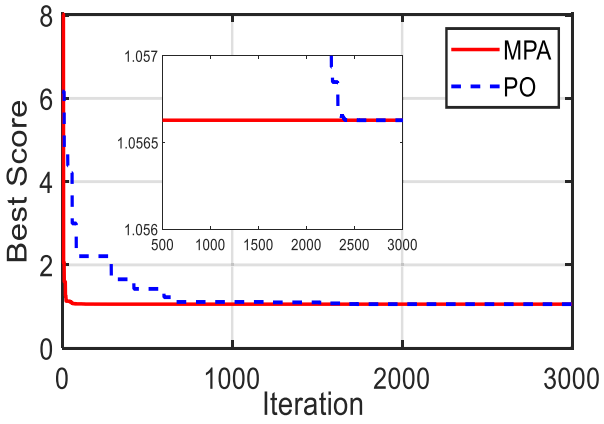

FIGURE 9. Convergence curve of MPA and PO optimization algorithms for the second case of SR-12PEM 500 W.

and is calculated as [11], [15], [29]:

$$C_{O_2} = \frac{P_{O_2}}{5.08 \times 10^6 \times e^{-\left(498/T\right)}} \tag{12}$$

The ohmic loss V_{ohmic} is calculated depending on the fundamentals of Ohm's law and directly depends on the current density, and it can be written as the following:

$$V_{ohmic} = I_{fc}\left(R_M + R_C\right) \tag{13}$$

where R_M and R_c present the resistance of the membrane and the equivalent resistance that the protons face when transported through the membrane and it is considered as a constant value. Accordingly, the resistance of the membrane surface can be given from the following expression:

$$R_M = \frac{\rho_M l}{A} \tag{14}$$

where l denotes the effective thickness of the membrane surface (cm), A is the area of the membrane surface (cm^2), and ρ_M denotes the resistivity of the membrane against the flow of electrons (Ω.cm) and is calculated empirically for Nafion membrane from the following expression [12], [27], [28]:

$$\rho_M = \frac{181.6\left[1 + 0.03\left(\frac{I_{fc}}{A}\right) + 0.062\left(\frac{T}{303}\right)^2\left(\frac{I_{fc}}{A}\right)^{2.5}\right]}{\left[\lambda - 0.634 - 3\left(\frac{I_{fc}}{A}\right)\right] \times \exp\left[4.18\left(\frac{T-303}{T}\right)\right]} \tag{15}$$

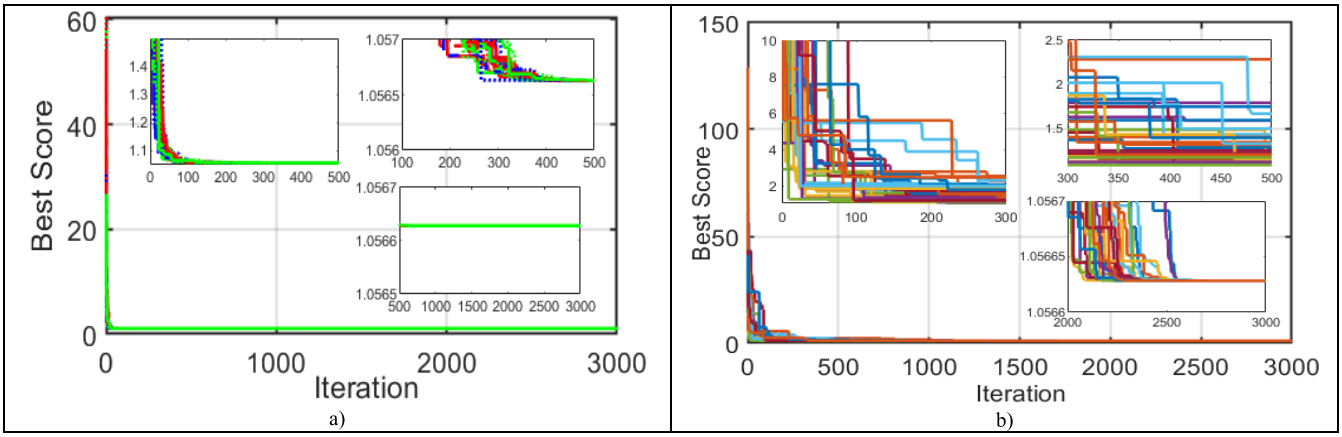

FIGURE 10. Convergence trends of the fitness function over the 30 runs for application a) MPA and b) PO with case of SR-12PEM 500 W.

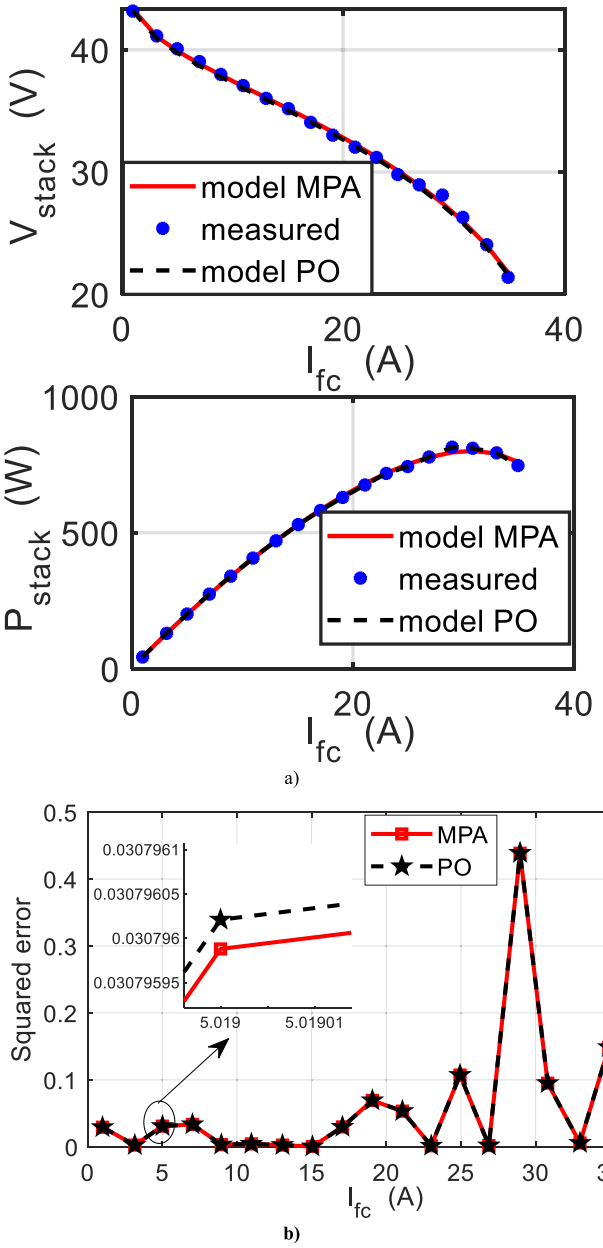

FIGURE 11. a) The I/V and I/P curve characteristics and b) Squared error between the estimated and measured data of SR-12PEM 500W based on MPA optimization algorithm.

where λ denotes to an adjustable parameter, which indicates the water content of the membrane material. The value of λ can be adjusted between 13 and 24 [9], [10].

The last part of these losses is the concentration voltage drop V_{con}, which appears due to the changes in the concentration of hydrogen and oxygen or fuel crossover and is calculated according to the following expression:

$$V_{con} = -\beta \ln\left(1 - \frac{J}{J_{\max}}\right) \tag{16}$$

where β denotes the adjusting parametric coefficient; J and J_{max} denote the current density and the maximum current density (A cm^{-2}), respectively.

C. OBJECTIVE FUNCTION

From the mathematical expressions described by equations (4-16), it is obviously noticed that the operation and performance characteristics of the PEMFC stack system are originally depended on a number of parameters. A part of these parameters are not available in the datasheet of the manufacturer and have to be carefully estimated to guarantee an accurate representation of the PEMFC, which gives results that match with experimental data. After the closer study of the above-mentioned equations, it is found that a set of parameters (ξ_1, ξ_2, ξ_3, ξ_4, β, R_c *and* λ) are not recognized in the datasheet and have to be extracted. The degree of matching between the model of the PEMFC and the experimental data is obtained by calculating the differences between the output voltage of the proposed model and that measured experimentally under different operating currents. In this paper, the sum of squared errors (SSE) between the measured values of voltage and the values of the output voltage of the PEMFC model is considered as the objective function (OF). The objective function to minimize the SSE is commonly used in many works of literature [8], [9], [14] is expressed by the following:

$$OF = \min SSE(X) = \sum_{i=1}^{N} (V_{meas} - V_{est})^2 \tag{17}$$

The objective function of (17) is ruled by the following constraints:

$$\begin{aligned} \xi_{k\min} \le \xi_k \le \xi_{k\max}, \quad k = 1:4 \\ \beta_{\min} \le \beta \le \beta_{\max} \\ R_{C\min} \le R_C \le R_{C\max} \\ \lambda_{\min} \le \lambda \le \lambda_{\max} \end{aligned} \tag{18}$$

where X is a vector of the seven unknown parameters that have to be determined, V_{meas} is the output voltage obtained experimentally from actual PEMFC, V_{est} is the output voltage obtained from the proposed model and N is the length of the experimental data series used for validation. MPA and PO methods are proposed for determining the optimal values of these parameters of the PEMFC model to give a high agreement with the results of the actual fuel cell stacks.

III. MPA

The proposed Marine Predators Algorithm (MPA) has been introduced by Faramarzi *et al.* [24]. The MPA has been implemented to imitate the strategy of foraging optimally for the Marine Predators (MP) to detect their *Prey* as the following: In the case of a low concentration of prey, the MP follow the Lévy behavior. In the case of abundant *Prey*, the MP follow the Brownian movements' behavior [24], [30]. According to the environmental effects, the velocity-ratio v from the *Prey* to MPA can be changed based on the behaviors of Lévy and Brownian as follows:

- In the low velocity-ratio $v < 0.1$, the most suitable behavior for MP is Lévy. On the other hand, the *Prey* is proceeding in Brownian/Lévy behavior;

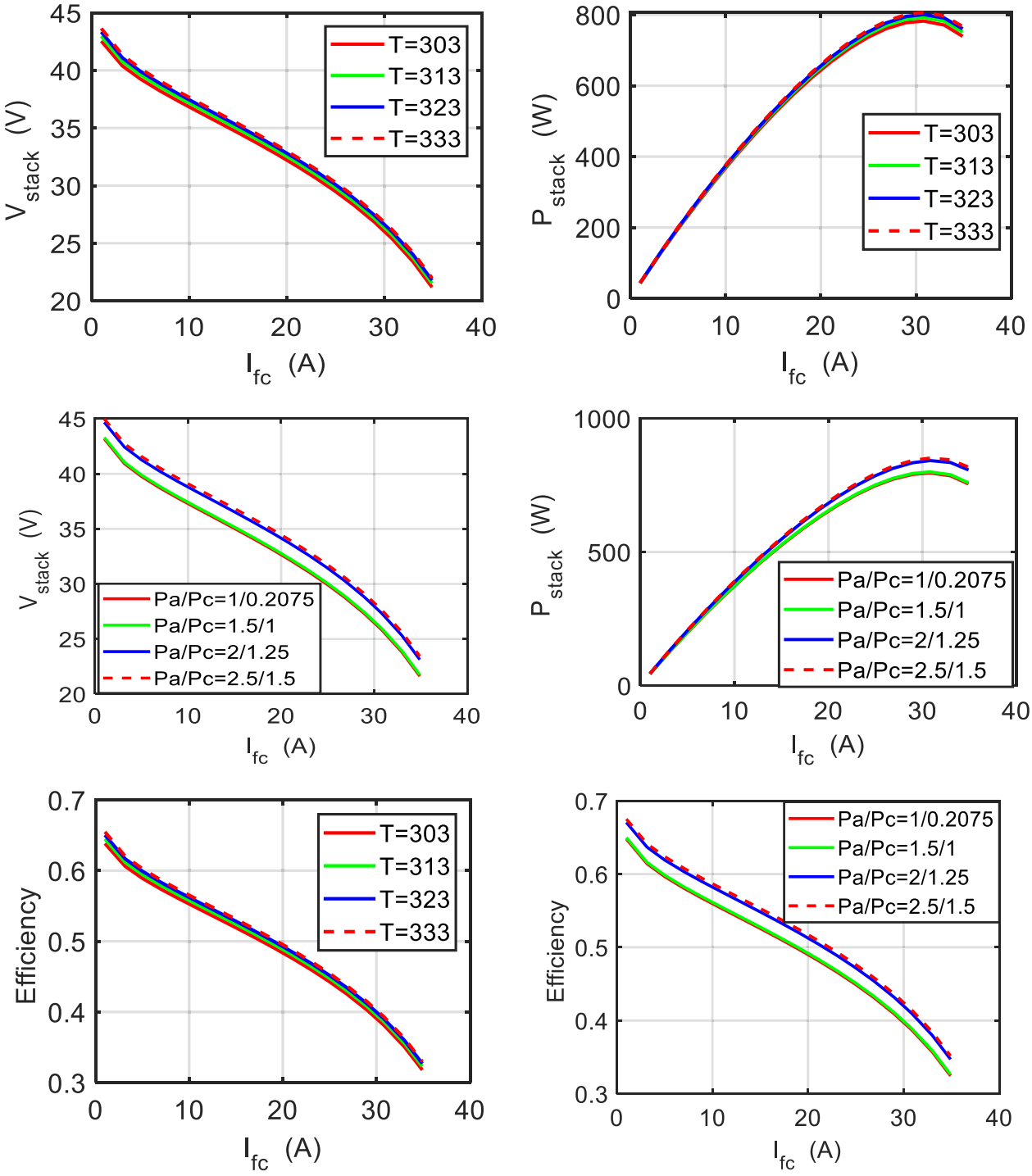

FIGURE 12. Characteristics of SR-12PEM 500 W with the variation of the Temperature and pressure based on MPA optimization algorithm.

- In the low velocity-ratio $v = 1$, in the case of the *Prey* can move in Lévy behavior, therefore the MP have to follow the Brownian behavior;
- In the high velocity-ratio $v > 10$, the most suitable behavior for MP is to be without moving. On the other hands, the *Prey* is proceeding in Brownian/Lévy behavior.

The scheme of the MPA methodology can be proposed in the following steps:

Firstly, the *Prey* in a group can be initiated through a search-space based on formula (19):

$$X_0 = X_{\min} + rand(X_{\max} - X_{\min}) \tag{19}$$

where X_{min} and X_{max} represent the lower & upper boundaries and rand is a random number that take a range from 0 to 1.

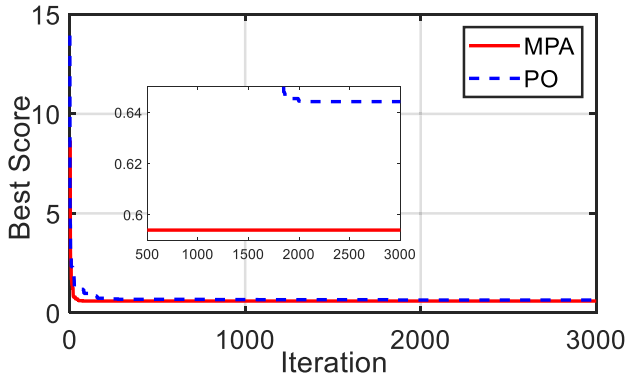

FIGURE 13. Convergence curve of MPA and PO optimization algorithms for the third case of study of 250 W stack.

Then, the fitness of MP can be determined. According to ≪*the survival of the fittest theory*≫, the fittest solution is considered as a top MP to structure a matrix that can be defined as *Elite*.

The *Elite* matrix can be represented in the following form:

$$Elite = \begin{bmatrix} X^I_{1,1} & X^I_{1,2} & \dots & X^I_{1,d} \\ X^I_{2,1} & X^I_{2,2} & \dots & X^I_{2,d} \\ : & : & : & : \\ X^I_{n,1} & X^I_{n,2} & \dots & X^I_{n,d} \end{bmatrix} \quad (20)$$

where $\overrightarrow{X^I}$ introduces the top MP vector, in addition, it is reproduced n times to construct an n×d *Elite* matrix. n is the agents' number and d is the dimensions' number.

The MP can update their locations based on the *Prey* metrics with the same dimensions as *Elite*. The *Prey* metrics is as follows:

$$prey = \begin{bmatrix} X^I_{1,1} & X^I_{1,2} & \dots & X^I_{1,d} \\ X^I_{2,1} & X^I_{2,2} & \dots & X^I_{2,d} \\ : & : & : & : \\ X^I_{n,1} & X^I_{n,2} & \dots & X^I_{n,d} \end{bmatrix} \quad (21)$$

The main iteration-loop of the MPA can be provided into three-phases depending on the velocity-ratio that are presented as follows:

A. EXPLORATION-PHASE

This phase occurs in high velocity-ratio, and it can be written as follows:

$$while\ Iter < \frac{1}{3} \cdot Max\_Iter$$

$$\overrightarrow{stepsize_i} = \overrightarrow{R_B} \otimes (\overrightarrow{Elite_i} - \overrightarrow{R_B} \otimes \overrightarrow{Prey_i}), \quad i = 1, .., n \quad (22)$$

$$\overrightarrow{Prey_i} = \overrightarrow{Prey_i} + P \cdot \overrightarrow{R} \otimes \overrightarrow{stepsize_i} \quad (23)$$

where R_B is a vector of random numbers and it depends on the nominal distribution introducing the Brownian movement. "⊗" provides the entry wise multiplications. $P = 0.5$ and it is constant. R is a random numbers vector that takes a range [0, 1]. This phase takes place in the one-third of iterations when the step-size or the velocity of motion is high for high exploration ability. "*Iter*" is the present iteration.

B. INTERMEDIATE-PHASE

This phase occurs in unit velocity-ratio. The exploration is gradually changed to exploitation and it is proposed as follows:

$$while\ \frac{1}{3} \cdot Max\_Iter < Iter < \frac{2}{3} \cdot Max\_Iter$$

-In the first-half of the population:

$$\overrightarrow{stepsize_i} = \overrightarrow{R_L} \otimes (\overrightarrow{Elite_i} - \overrightarrow{R_L} \otimes \overrightarrow{Prey_i}), \quad i = 1, .., n/2 \quad (24)$$

$$\overrightarrow{Prey_i} = \overrightarrow{Prey_i} + P \cdot \overrightarrow{R} \otimes \overrightarrow{stepsize_i} \quad (25)$$

-In the second-half of the population:

$$\overrightarrow{stepsize_i} = \overrightarrow{R_B} \otimes (\overrightarrow{R_B} \otimes \overrightarrow{Elite_i} - \overrightarrow{Prey_i}), \quad i = 1, .., n/2, n \quad (26)$$

$$\overrightarrow{Prey_i} = \overrightarrow{Elite_i} + P \cdot CF \otimes \overrightarrow{stepsize_i} \quad (27)$$

where $\overrightarrow{R_L}$ is proposed based on the Lévy-flight behavior. In the intermediate-phase, the first half of *Prey* can proceed with Lévy steps. On the other hand, the second half utilizes Brownian steps. The *CF* is considered as an adaptive parameter to control the step-size of MP motions. The CF can be determined by the following Eq. (28):

$$CF = (1 - \frac{Iter}{Max\_Iter})^{(2\frac{Iter}{Max\_Iter})} \quad (28)$$

C. EXPLOITATION-PHASE

This phase occurs in low velocity-ratio and it is prepared as follows:

$$while\ Iter > \frac{2}{3} \cdot Max\_Iter$$

$$\overrightarrow{stepsize_i} = \overrightarrow{R_L} \otimes (\overrightarrow{R_L} \otimes \overrightarrow{Elite_i} - \overrightarrow{Prey_i}), \quad i = 1, .., n \quad (29)$$

$$\overrightarrow{Prey_i} = \overrightarrow{Elite_i} + P \cdot CF \otimes \overrightarrow{stepsize_i} \quad (30)$$

One of the critical points that can be taken into consideration is the manner of the MP can be affected by environmental problems like the eddy formation or Fish Aggregating Devices (FADs). According to [24], the MP consume 80% of their time in the vicinity of FADs looking for the *Prey*. The rest of MP time is consumed in another environment to find their *Prey*. In search space, the FADs effects are considered as trapping. Thereby, the FADs are deemed as local optima. The FADs process is formulated as follows:

If $r < FADs$

$$\overrightarrow{Prey_i} = \overrightarrow{Prey_i} + CF[\overrightarrow{X}_{\min} + \overrightarrow{R} \cdot (\overrightarrow{X}_{\max} - \overrightarrow{X}_{\min})] \otimes \overrightarrow{U} \quad (31)$$

If $r > FADs$

$$\overrightarrow{Prey_i} = \overrightarrow{Prey_i} + [FADs(1 - r) + r](\overrightarrow{Prey_{r1}} - \overrightarrow{Prey_{r2}}) \quad (32)$$

where FADs = 0.2 is the impact of FADs on the optimization process. $\overrightarrow{U}$ is the binary with the arrays having 0 and 1. r is

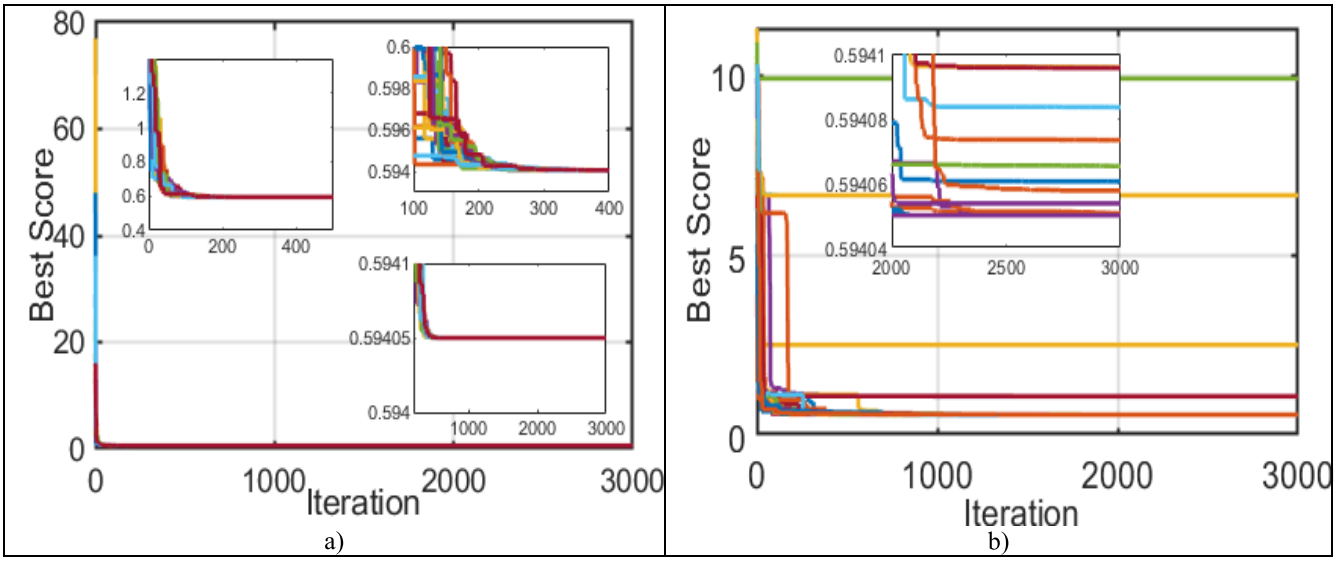

FIGURE 14. Convergence trends of the fitness function over the 30 runs for application a) MPA and b) PO with case of 250 W stack.

a random number in [0,1]. $\overrightarrow{X}_{\max}$ and $\overrightarrow{X}_{\min}$ are including the lower and upper boundaries of the dimensions. r_1 and r_2 are random indexes of *Prey* matrix. MPA has a well memory that can be useful to remember the old positions of the *Prey*. Therefore, based on the fitness values, each present and old solutions can be compared, and the best one can be saved at each iteration.

The MPA implementation procedure can be summarized in the flowchart shown in Fig. 2.

IV. PO

The proposed PO technique is considered as a physics-based algorithm combined with swarm-based characteristics which are concerned mainly with finding global optima. The PO has been implemented by Q. Askari *et al.* [25], and it has been inspired by the different phases of the Politics process. Politics process can be divided into two main attitudes: every individual optimizes its good-will to win the election, and every party attempt to find the maximum number of seats in parliament to form a government. However, the PO is created as a consequence of five-phases involving party formation and constituency allocation, election campaign, party switching, inter-party election, and parliamentary affairs [25].

The scheme of the PO methodology can be proposed in the following process using the variables that defined in Table 1 [25]:

Firstly, the phase of party formation and constituency allocation executes only once for the purpose of initialization and the others of the four-phases perform in a loop.

A. PARTY FORMATION AND CONSTITUENCY ALLOCATION

The β is sectioned into n political parties. Every party β_i is composed of n members. Every j^{th} member p_i^j is deemed as a potential solution. This potential solution can represent as an election candidate. It is supposed n constituencies, and j^{th} member of every party contests election from the j^{th} constituency C_j.

The fittest member of a party is expressed as the party leader. The election of the party leader is determined using (33) as follows:

$$q = \arg\min_{1\le j\le n} f(p_i^j), \quad i = 1, \ldots, n$$
$$and,\ p_i^* = p_i^q \tag{33}$$

Therefore, all the party leaders' β^* can be introduced by (34) as the following expression:

$$\beta^* = \left\{p_1^*, p_2^*, p_3^*, ..., p_n^*\right\} \tag{34}$$

$$p_{i,k}^j(t+1) = \begin{cases} m^* + r\left(m^* - p_{i,k}^j(t)\right), & \text{if } p_{i,k}^j(t-1) \le p_{i,k}^j(t) \le m^* \text{ or } p_{i,k}^j(t-1) \ge p_{i,k}^j(t) \ge m^* \\ m^* + (2r-1)\left|m^* - p_{i,k}^j(t)\right|, & \text{if } p_{i,k}^j(t-1) \le m^* \le p_{i,k}^j(t) \text{ or } p_{i,k}^j(t-1) \ge m^* \ge p_{i,k}^j(t) \\ m^* + (2r-1)\left|m^* - p_{i,k}^j(t-1)\right|, & \text{if } m^* \le p_{i,k}^j(t-1) \le p_{i,k}^j(t) \text{ or } m^* \ge p_{i,k}^j(t-1) \ge p_{i,k}^j(t) \end{cases} \tag{36}$$

$$p_{i,k}^j(t+1) = \begin{cases} m' + (2r-1)\left|m' - p_{i,k}^j\right|, & \text{if } p_{i,k}^j(t-1) \le p_{i,k}^j(t) \le m^* \text{ or } p_{i,k}^j(t-1) \ge p_{i,k}^j(t) \ge m' \\ p_{i,k}^j(t-1) + r\left(p_{i,k}^j(t) - p_{i,k}^j(t-1)\right), & \text{if } p_{i,k}^j(t-1) \le m^* \le p_{i,k}^j(t) \text{ or } p_{i,k}^j(t-1) \ge m^* \ge p_{i,k}^j(t) \\ m^* + (2r-1)\left|m^* - p_{i,k}^j(t-1)\right|, & \text{if } m^* \le p_{i,k}^j(t-1) \le p_{i,k}^j(t) \text{ or } m^* \ge p_{i,k}^j(t-1) \ge p_{i,k}^j(t) \end{cases} \tag{37}$$

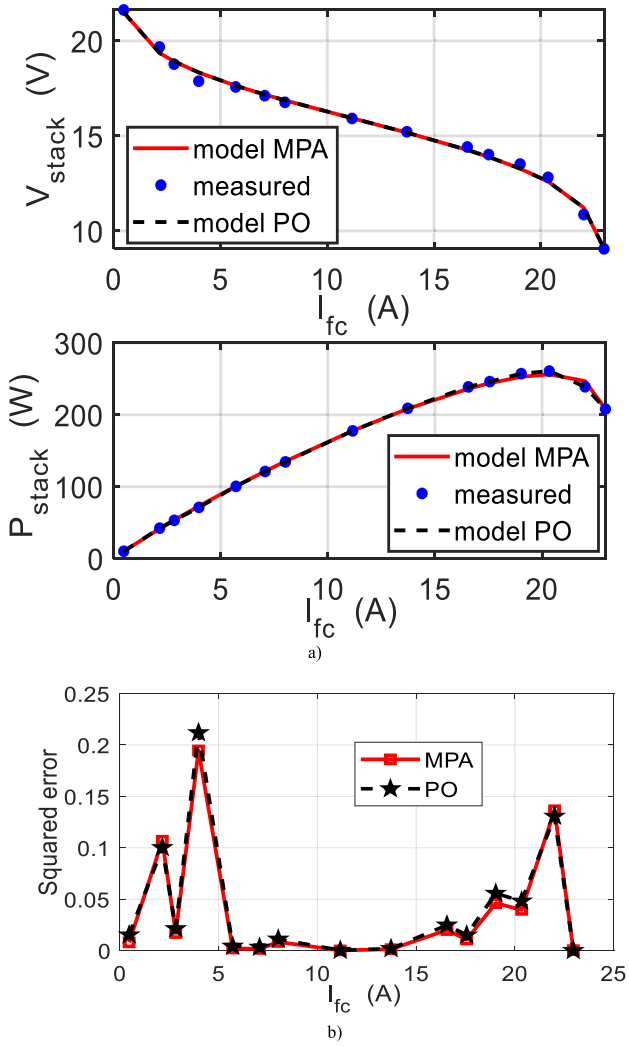

FIGURE 15. a) The I/V and I/P curve characteristics and b) Squared error between the estimated and measured data of 250 W stack based on MPA and PO algorithms with case of 250 W stack.

After selection, the winners from all the constituencies become the parliamentarians C^* as shown in (35) as the following formula:

$$C^* = \{c_1^*, c_2^*, c_3^*, ..., c_n^*\} \tag{35}$$

B. ELECTION CAMPAIGN "EXPLORATION AND EXPLOITATION"

This phase-step assists nominees to make their performance better in the election. In this regard, there are three parts in this phase as following:

- A new position updating strategy called ≪recent past-based position updating strategy (RPPUS)≫ that can produce a suitable learn from the previous election. This strategy can be written by (36) and (37), as shown at the bottom of the previous page.
- The impact of the vote-bank of the party leader is delineated by updating the members' position.

TABLE 1. The variables definitions of the political-phases process.

Variable	Definition
β_i	ith political party
p_i^j	jth member of ith party
$\beta_{i,k}^j$	kth dimension of jth member of ith political party
C_j	jth constituency
p_i^*	leader of ith political party
c_j^*	winner of jth constituency
λ	party switching rate
n	variable number in each party
T_{max}	total number of iterations

- The comprehensive analysis with the constituency winner is proposed mathematically based on the updating of the candidate position.

C. PARTY SWITCHING (BALANCING EXPLORATION AND EXPLOITATION)

In this phase, an adaptive factor λ ≪party switching rate≫ is decreased in linear form from its maximum value to 0 during the iterations process. The probabilistic selection of p_i^j is turned to few randomly elected party β_r that can be changed with the least fit p_r^q of that party. The calculation of q index of β_r can be written as follows:

$$q = \underset{1 \le j \le n}{\arg\max}\ f(p_r^j) \tag{38}$$

D. ELECTION (FITNESS DETERMINATION)

The election is imitated by estimating the fitness of all the candidates contesting in a constituency and proclaiming the winner. In this process, c_j^* indicates the winner of j^{th} constituency (C_j). This phase can be modeled mathematically by (39) as the following expression:

$$\begin{aligned} q &= \underset{1 \le i \le n}{\arg\min}\ f(p_i^j) \\ c_j^* &= p_q^j \end{aligned} \tag{39}$$

E. PARLIAMENTARY AFFAIRS (EXPLOITATION AND CONVERGENCE)

The government is created, in accordance with an inter-party election. The party leaders and the constituency winners are made a decision by applying (33) and (39). Every winner c_j^* renews its position with reference to a randomly selected winner c_r^* and if it causes any modification in fitness of c_j^* thereafter the situation and fitness of c_j^* are renewed.

The PO implementation procedure can be summarized in the flowchart shown in Fig. 3 [25].

V. RESULTS

The simulation tests have been carried out to validate the applied optimization algorithms (MPA and PO). Both algo-

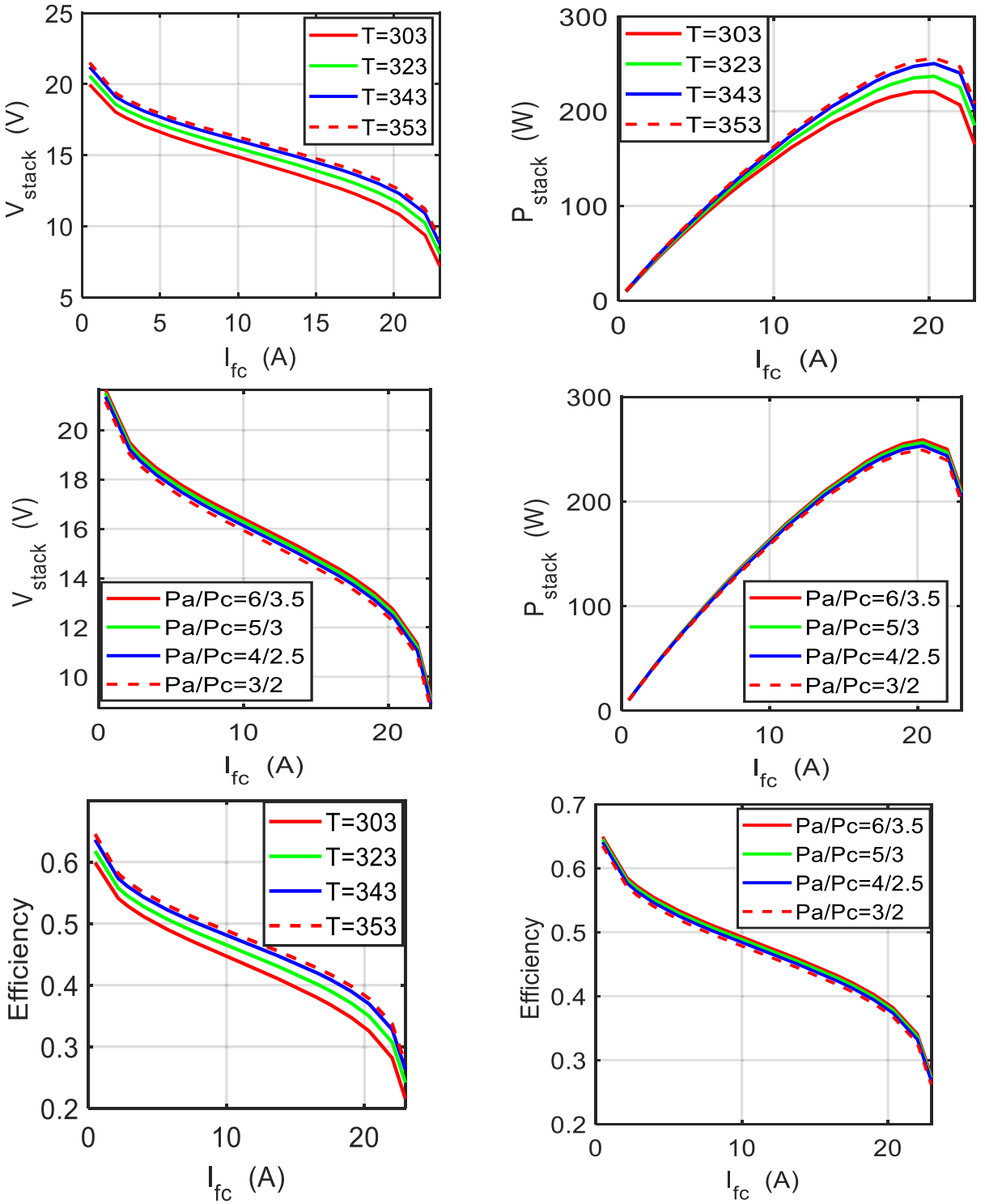

FIGURE 16. Characteristics of 250 W stack with the variation of the temperature and pressure based on MPA optimization algorithm.

rithms have been applied for estimating the parameters of PEM fuel cells. The two algorithms have been tested for estimating the parameters of three different modules of fuel cells, namely BCS 500W, SRR_12 modular, and 250W stack. The datasheet parameters of these commercial PEMFC stacks are obtained from [9]–[11], [14], [15], [22] and are presented in Table 2. Moreover, the estimated model parameters are ξ_1, ξ_2, ξ_3, ξ_4, β, R_C, and λ in PEMFC, as shown in Fig. 4.

The upper and lower limits of the unknown parameters for all case studies are given in [8], [10], [18], and [19] and presented in Table 2 (last three columns in the right).

TABLE 2. Parameters of the commercial PEMFC stacks and the search range of the unknown parameters.

Datasheet parameters				Search ranges		
FC stack type	BCS 500W	SR-12 modular	250 W stack	Parameter	Minimum	Maximum
N (cells)	32	48	24	ξ_1	-1.1997	-0.08532
A (cm^2)	64	62.5	27	$\xi_2 \times 10^{-3}$	0.8	6.00
l (μm)	178	25	178	$\xi_3 \times 10^{-5}$	3.60	9.80
J_{max} (A/cm^2)	0.469	0.672	0.680	$\xi_4 \times 10^{-4}$	-2.60	-0.954
P_{H2} (atm)	1	1.47628	1	Λ	10.00	24.00
P_{o2} (atm)	0.2075	0.2095	1	B	0.0136	0.5
T(K)	333	323	343	$R_C \times 10^{-4}$	1.00	8.00

TABLE 3. Parameter fitting results of BCS 500W based on PO and MPA optimization techniques; the bold Results are the best for MPA.

Parameter	PO	MPA	MAEO [22], 2020	GWO [15], 2017	SSO [18], 2019	CS-EO [20], 2019	HHO [31]; 2019
ξ_1	-1. 1997	**-0.986409267**	-0.85596	-1.018	-1.018	-1.1365	-1.165963
$\xi_2 \times 10^{-3}$	4.04218	**2.608509**	2.73328	2.3151	2.3151	2.9254	3.09095335
$\xi_3 \times 10^{-5}$	9.79980616	**3.6**	6.63428	5.2400	5.2400	3.7688	8.1088029
$\xi_4 \times 10^{-4}$	-1.9289267	**-1.92892845**	-1.92816	-1.2815	-1.2815	-1.3949	-1.8046841
Λ	20.8180558	**20.8167**	-1.92816	18.8547	18.8547	18.5446	19.3423812
B	0.0161136221	**0.01611354**	20.702572	0.0136	0.0136	0.0136	0.013601616
$R_C \times 10^{-4}$	1	**1**	0.016023	7.504	7.5036	8.000	6.490139
Min. Optimal	0.0115564179	**0.011556305**	0.01157	7.1889	7.1889	5.5604	0.059288512

Bold items indicate the best results and performance of the proposed MPA

The results of the two algorithms have been compared with each other and with those obtained using other techniques from the literature. Moreover, the optimized parameters using MPA and PO methods have been used to estimate the performance and characteristics of the PEMFC at different operating conditions. Furthermore, the characteristics have been compared with the measured data of each module.

For the simulation, a dedicated software program for fuel cell parameter extraction problem is developed in MATLAB for MPA and PO based upon their theories of operation which are described before. Simulations are performed using an Intel® core™ i5-4210U CPU, 1.7 GHz, 8 GB RAM Laptop.

A. PEMFC OF BCS 500W

To test and validate the proposed optimization algorithms, the proposed algorithms have been applied with the problem formulation PEM fuel cell of BCS 500W. The selected BCS 500W is studied because several studies have been introduced earlier for this purpose, but the majority have failed in achieving an accurate estimation for the parameters. The results of applying the MPA and PO algorithms to estimate the finest values of BCS 500W stack parameters are illustrated in Table 3. As shown from the table, the results gained by the MPA are better than those obtained by the PO technique and also are better than the other methods from literature. The convergence curves of the MPA and PO have been shown in Fig. 5, which reports that the MPA has the best convergence curve with respect to the speed of convergence and reaches the best minimum value of the objective function. From this figure, the MPA optimization algorithm reaches a minimum value of 0.011556305 while the PO reaches its minimum, which equal to 0.0115564179. It should be noted that the small difference between the results of the two algorithms. Table 3 shows the comparison between the estimated parameters of the PEMFC model using MPA and PO and other techniques. The results of MPA is the best one as compared with the latest published papers in the literature [22].

To validate more the effectiveness of MPA and PO optimization algorithms, the obtained results have been used to estimate the characteristics of the PEMFC by estimating the voltage and power curves versus the current. Furthermore, the estimated characteristics have been compared with the measured one for both models of MPA and PO as shown in Fig. 6. Figure 6.a) shows a very good match between the estimated and measured characteristics. It should be noted that the coincidence of the two curves of the estimated models of MPA and PO with the measured one because the values of SSE for MPA and PO are 0.0115564179 and 0.011556305, respectively. Additionally, figure 6.b) shows the squared error for both models based on MPA and PO techniques. Also, Table 4 listed the squared error between the estimated and measured performance of BCS 500w based on PO and MPA. Table 4 listed the obtained results of the estimated voltage using models based on MPA and PO algorithms and the squared error at each current value. Moreover, the characteristics of the PEMFC have been plotted at different operating condition of the pressure of PH2 /PO2 of 1.000/ 0.2075bar, 1.5/1.0bar, 2.0/1.25 and 2.5/1.5bar; and temperature of 303K, 313K, 323K and 333K as shown from Fig. 7 for only the MPA-based model.

As known, the performance of these algorithms is based on randomness and the sole best fitness value (SSE) in one of the runs cannot assure the acceptable performance of the optimization algorithms. As mentioned earlier, there is no

TABLE 4. Squared error between the estimated and measured performance of BCS 500W based on PO and MPA.

Measured Current (A)	Measured Voltage (V)	Estimated Voltage PO (V)	Squared Error for PO	Estimated Voltage MPA (V)	Squared Error for MPA
0.6	29	28.99635119	1.33E-05	28.99635196	1.33E-05
2.1	26.31	26.30648909	1.23E-05	26.30648852	1.23E-05
3.58	25.09	25.09457646	2.09E-05	25.09457577	2.09E-05
5.08	24.25	24.25586117	3.44E-05	24.25586063	3.43E-05
7.17	23.37	23.37676881	4.58E-05	23.37676859	4.58E-05
9.55	22.57	22.58594898	0.00025437	22.58594912	0.000254375
11.39	22.06	22.06176806	3.13E-06	22.06176843	3.13E-06
12.54	21.75	21.75964976	9.31E-05	21.75965023	9.31E-05
13.73	21.45	21.46236454	0.000152882	21.46236507	0.000152895
15.73	21.09	20.98867838	0.010266071	20.98867892	0.01026596
17.02	20.68	20.69532738	0.000234929	20.69532788	0.000234944
19.11	20.22	20.23159646	0.000134478	20.23159678	0.000134485
21.2	19.76	19.77133501	0.000128483	19.77133503	0.000128483
23	19.36	19.36622712	3.88E-05	19.36622682	3.88E-05
25.08	18.86	18.86646464	4.18E-05	18.86646397	4.18E-05
27.17	18.27	18.27457202	2.09E-05	18.27457124	2.09E-05
28.06	17.95	17.95314979	9.92E-06	17.95314925	9.92E-06
29.26	17.3	17.29287158	5.08E-05	17.29287241	5.08E-05
		SSE PO	1.16E-02	**SSE MPA**	1.16E-02

guarantee that the algorithms can repeat the same results overruns. In order to appreciate the stability and accurateness as well as give a clear assessment of the proposed MPA and PO in obtaining the exact values of PEMFC unknown parameters, sensitivity and statistical analysis is studied for all tested PEMFC stacks. Fig. 8 shows the convergence curve of 30 independent runs. From the figure, over the 30 runs; the MPA reached the same optimized solution while the PO algorithm results are varying each run around its best solution. The results are very essential which prove that the MPA is stability and reliability of the MPA.

Statistical analysis is completed for assurance and valuation the robustness concert of the optimization algorithms. So, MPA and PO algorithms are performed 30 individual runs. The finest objective function is logged and stated. Furthermore, statistical indices of Mean, Standard deviation (SD), relative Error (RE), root mean square error (RMSE), the minimum and maximum over 30 runs are calculated. The results of MPA and PO algorithms are recorded in Table 5. The listed results of the table demonstrate that the MPA technique has the best performance during this test while the value of SD, RE and RMSE of the PO algorithm is relatively high as shown from the table because it fails to optimize the problem in number of runs. So, the MPA is an effective algorithm for solving the optimization problem of parameters' identification of various mathematical models of BCS 500W.

Furthermore, the Wilcoxon signed-rank test is performed to validate the MPA and PO algorithms. The reported results are listed in Table 5. The results show that P-value for both

TABLE 5. Statistical measurement of the proposed MPA and PO methods for BCS 500W based on 30 individual runs.

	MPA Model	**PO Model**
Min	0.0116	0.0116
Max	0.0116	0.1881
Mean	0.0116	0.0188
Median	0.0116	0.0116
SD	6.2747e-15	3.2161
RE	3.8879e-13	18.7596
MAE	1.4976e-16	0.0072
RMES	1.6197e-16	0.0324
Eff.	100	90.3679
	WILCOXON SIGNED RANK TEST	
P	1.6869e-06	1.7344e-06
Rank	1	1

algorithms MPA and PO are 1.6869e-06 and 1.7344e-06, respectively. Moreover, Ranke is 1 both algorithms. At the default 5% significance level, the value h = 1 designates that the test rejects the null hypothesis of zero medians. P-values in Table 8 which are produced based on Wilcoxon test demonstrate that the results of MPA and PO algorithms are statistically significant.

B. SR-12PEM 500 W

The second case of study is applied to estimate the model parameters of the SR-12PEM 500 W. The parameters and data

TABLE 6. Parameter fitting results of SR-12PEM 500 W based on PO and MPA optimization techniques; the bold Results are the best for MPA.

Parameter	PO	**MPA**	MAEO [22], 2020	HGWO [23], 2020	GWO [15], 2017	SSO [18], 2019	SC-EO [20], 2019
ξ_1	-0.8600196	**-1.028359**	-0.86068	-1.0349	-0.9664	-0.9664	-1.0353
$\xi_2 \times 10^{-3}$	3.37581909	**3.898047**	2.77134	3.3498	2.2833	2.2833	3.3540
$\xi_3 \times 10^{-5}$	9.79375167	**9.799999**	6.169649	7.2386	3.40	3.40	7.2428
$\xi_4 \times 10^{-4}$	-0.9540	**-0.954**	-0.954009	0.9529	-0.95400	-0.9540	-0.9540
Λ	22.9999999	**23**	22.98870	10	15.7969	15.7969	10
B	0.17532026	**0.1753203**	0.175366	0.1462	0.1804	0.1804	0.1471
$R_C \times 10^{-4}$	6723109	**6.7231067**	6.70732	7.0936	6.6853	6.6853	7.1233
Min. Optimal	1.05662833403	**1.05662833402**	1.05663	7.5646	1.517	1.517	7.5753

Bold items indicate the best results and performance of the proposed MPA

TABLE 7. Squared error between the estimated and measured performance of SR-12PEM 500W based on PO and MPA.

Measured Current (A)	Measured Voltage (V)	Estimated Voltage PO (V)	Squared Error for PO	Estimated Voltage MPA (V)	Squared Error for MPA
1.004	43.17	43.34080925	0.029175801	43.34080934	0.02917583
3.166	41.14	41.09007769	0.002492237	41.09007778	0.002492228
5.019	40.09	39.91451205	0.030796021	39.91451214	0.030795988
7.027	39.04	38.85715212	0.033433347	38.85715222	0.033433311
8.958	37.99	37.93346469	0.003196242	37.93346479	0.00319623
10.97	37.08	37.01453672	0.004285441	37.01453682	0.004285427
13.05	36.03	36.07990554	0.002490563	36.07990565	0.002490574
15.06	35.19	35.17136395	0.000347302	35.17136405	0.000347298
17.07	34.07	34.2420883	0.029614382	34.2420884	0.029614418
19.07	33.02	33.28312599	0.069235288	33.2831261	0.069235343
21.08	32.04	32.27070019	0.053222578	32.27070029	0.053222625
23.01	31.2	31.23769365	0.001420811	31.23769375	0.001420819
24.94	29.8	30.12737151	0.107172103	30.1273716	0.107172164
26.87	28.96	28.91713394	0.001837499	28.91713402	0.001837492
28.96	28.12	27.45775678	4.39E-01	27.45775686	0.438565982
30.81	26.3	25.99180452	0.094984452	25.99180458	0.094984416
32.97	24.06	23.98486896	0.005644674	23.98486899	0.005644669
34.9	21.4	21.78563391	0.148713516	21.78563392	0.148713519
		SSE PO	**1.056628334**	**SSE MPA**	**1.056628334**

specification of the SR-12PEM 500 W are listed in Table 2. The results of the estimated parameters have been listed in Table 6. Also, Table 4 consists of a comparison between the PO and MPA algorithms and with the obtained results by other researchers. From the table, the best solution has been reached by the MPA and equals 1.056628334025551 while the best optimal value with the PO is 1.056628334030994. Moreover, the table shows that the other researchers with other optimization techniques could not reach the same solution. Furthermore, a comparison between PO and MPA with respect to the convergence characteristics has been shown in Fig. 9. The figure shows that the convergence speed of the MPA is better than that of the PO.

The simulation tests have been done to test and evaluate the robustness of the MPA and PO optimization techniques with this case of study. The MPA and PO have been applied for 30 runs. The convergence curves of the 30 runs have been shown in Fig. 10 for both algorithms. The figure shows that the MPA has the ability to reach the same best solution over 30 runs while figure10.b) shows the PO algorithm reaches to different values of the best solution in the number of runs. This concludes that the MPA is the best choice for estimating the parameters of the PEMFC model.

The results of the characteristics of SR-12PEM 500 W based on the estimated parameters using MPA and PO and the experimental data have been shown in Fig. 11.a). The figure shows that the obtained characteristics from the proposed MPA optimization algorithm introduce a high matching degree with the experimental data. Furthermore, the squared error between the measured voltages and the estimated based on MPA and Po algorithms have been illustrated in figure 11.b) and table 7. Moreover, due to the Exploration and exploitation characteristics of MPA, which is related to global search; the MPA keeps improving a longer time than PO.

Statistical results of the applied MPA and PO methods for SR-12PEM 500 W based on 30 individual runs have been

TABLE 8. Statistical measurement of the proposed MPA and PO methods for SR-12PEM 500W based on 30 individual runs.

	MPA Model	PO Model
Min	1.0566	1.0566
Max	1.0566	1.0809
Mean	1.0566	1.0579
Median	1.0566	1.0566
SD	1.2715e-13	0.5074
RE	1.1663e-13	0.0366
MAE	4.1078e-15	0.0013
RMES	4.2924e-15	0.0052
Eff.	100	99.8803
	WILCOXON SIGNED RANK TEST	
P	1.6805e-06	1.7333e-06
Rank	1	1

listed in table 8. The results show that the MPA and PO has good performance with an example SD of 1.2715e-13 and 0.5074 respectively, which confirms that the superior of MPA with the good performance of PO algorithm. Furthermore, the Wilcoxon signed-rank test is performed to validate the MPA and PO algorithms. The reported results are listed in Table 8. The results show that P-value for both algorithms MPA and PO are 1.6805e-06 and 1.7333e-06, respectively. Moreover, Ranke is 1 of both algorithms. At the default 5% significance level, the value h = 1 designates that the test rejects the null hypothesis of zero medians. P-values in Table 8 which are produced based on the Wilcoxon test demonstrate that the results of MPA and PO algorithms are statistically significant.

For more validating, the estimated model based on the MPA is used for plotting the characteristics at different operating conditions such as the variation of temperature and pressure, as shown in Fig. 12.

C. 250 W STACK

For more justification, the two algorithms of MPA and PO have been applied for extracting the model parameters of the 250 W stack. The data specifications of the 250 W stack have been listed in Table 2. The results of the estimated parameters have been concluded in Table 9. From the table; it is revealed that the MPA algorithm has the best result concerning reaching the minimum value of the objective function. The best optimal value of MPA is equal to 0.5940499653, while the best value with PO equals 0.644205811. Also, the table presents a comparison with other techniques from the literature. From the comparison, the optimal values of the objective function obtained by the MPA and PO are better than the other techniques.

In order to analyze the convergence characteristics of the two algorithms, the convergence curves of the PO and MPA algorithms via iterations have been shown in Fig. 13. The figure shows that the MPA has a better convergence speed of solving the optimization problem compared with the PO technique.

Another time, the robustness and probability of finding the optimal answer by the MPA and PO algorithms have been tested by finding the best solution of 30 independent runs. The results of these runs have been shown in Fig. 14. Figure 14.a) proves the robustness of the MPA optimization algorithm for finding the best parameters of the PEMFC model. While figure 14.b) shows the results of PO algorithm which confirms the results have been varied each run around the best one.

The validation of the results has been proved by plotting the voltage and power characteristics versus the current for both models of MPA and PO, as shown in Fig. 15. From the figure, the precise matching between the estimated characteristics and the experimental data of the fuel cell can be easily investigated. Table 10 shows the squared error between the estimated and measured performance of 250 W stack based on PO and MPA. Furthermore, Table 11 shows the statistical measurement of the planned MPA and PO methods for 250 W stack based on 30 individual runs. The statistical results prove that the both algorithms of MPA and PO have robust performance with consideration of superiority of the MPA algorithm. Furthermore, the characteristics of the module with the variation of the temperature and pressure have been shown through Fig. 16.

D. RESULTS DISCUSSION

In the previous sub-sections, the results of the application of both MPA and PO algorithms have been presented. The two algorithms have been applied to estimate three various cases of the PEMFC. The results started with the convergence

TABLE 9. Parameter fitting results of 250 W stack based on PO and MPA optimization techniques; the bold results are the best for MPA.

Parameter	PO	MPA	HHO [31], 2019	MAEO [22], 2020	HGWO [23], 2020	HADE [9], 2015	JAYA [19], 2019	CS-EO [20], 2019
ξ_1	-1.089330092	**-0.997571108**	-1.162001	-0.89119	-0.8521	-0.9440	-0.95200	-0.8532
$\xi_2 \times 10^{-3}$	3,6293684	**2.4028717**	4.01799947	2.264152	2.8132	3.0778	3.1000	2.8121
$\xi_3 \times 10^{-5}$	6.176176	**3.6**	9.74536802	3.84106	8.0946	7.8000	8.000	8.1180
$\xi_4 \times 10^{-4}$	-1.50913327	**-1.5543264149**	-1.3345217	-1.55950	-1.2619	-1.8800	-1.900	-1.2623
Λ	23.99999	**23.99999**	16.681058	22.9999	14.5104	23.000	23.000	14.4722
B	0.0547065105	**0.0559270605**	0.047836035	0.05454	0.035232	0.032672	0.03270	0.035251
$R_C \times 10^{-4}$	5	1	7.00847713	1.00019	1	1.000	1.000	1.000
Min. Optimal	0.644205811	**0.5940499653**	1.02274171	0.64202	8.0594	15.669	9.9010	8.0665

Bold items indicate the best results and performance of the proposed MPA

TABLE 10. Squared error between the estimated and measured performance of 250 W stack based on PO and MPA.

Measured Current (A)	Measured Voltage (V)	Estimated Voltage PO (V)	Squared Error for PO	Estimated Voltage MPA (V)	Squared Error for MPA
0.4717	21.63	21.50649273	0.015254046	21.54020798	0.008062607
2.149	19.68	19.36351472	0.100162932	19.35305278	0.106894484
2.83	18.78	18.92605721	0.021332709	18.91064631	0.017068459
3.983	17.88	18.34032262	0.21189691	18.32121836	0.194673642
5.713	17.58	17.64521602	0.004253129	17.62619327	0.002133819
7.075	17.12	17.1772021	0.003272081	17.1607316	0.001659063
8.019	16.77	16.87589607	0.011213978	16.86195321	0.008455393
11.16	15.92	15.93708236	0.000291807	15.9339441	0.000194438
13.73	15.22	15.17607284	0.001929595	15.18272296	0.001389578
16.56	14.42	14.26228618	0.02487365	14.27863521	0.019984003
17.56	14.02	13.89706788	0.015112307	13.91603434	0.010808858
19.03	13.52	13.28394272	0.055723042	13.30517558	0.046149531
20.34	12.82	12.60059404	0.048138973	12.62090883	0.039637293
22.01	10.86	11.22149147	0.130676082	11.22946236	0.136502437
22.96	9.058	9.06665469	7.49E-05	9.037110743	0.000436361
0.4717	21.63	21.50649273	0.015254046	21.54020798	0.008062607
2.149	19.68	19.36351472	0.100162932	19.35305278	0.106894484
2.83	18.78	18.92605721	0.021332709	18.91064631	0.017068459
		SSE PO	**0.644206146**	SSE MPA	**0.594049965**

curves of the two algorithms to solve the optimization problem. Then the minimum value of each algorithm has been presented and compared with those of other reported optimization algorithms. Considering the convergence characteristics, the MPA algorithm has the best one as confirmed from figures of the convergence curves. Moreover, MPA can reach in all studied cases to the finest value of the objective function as confirmed from tables 3, 4 and 5. While, the results of the PO are better than those of the other reported methods as shown from table 3, 4 and 5 but its results are the second ones after those of the MPA algorithms. So, the MPA and PO algorithms have the ability to solve the presented optimization problem to estimate the parameters of PEMFC with the superiority of the MPA algorithm.

Furthermore, the obtained optimized parameters have been used to estimate the V/I and P/I characteristics of the studied PEMFC cases. The obtained results based on the MPA and PO estimated parameters confirm the coincide of the estimated PEMFC characteristics with those of the measured and datasheet.

The merits of the MPA can be shown by focusing on the MPA flowchart of figure 2. The MPA algorithm has three phases that improve its characteristics of global solution (exploration) w.r.t the first and second phases and local solution (exploitation) considering the third phase which enhances its characteristics when MPA applied 30 individual runs with the same obtained results. Although its limitation can be well-thought-out in the future work once it applies for more complex optimization problems with large a variable.

TABLE 11. Statistical measurement of the proposed MPA and PO methods for 250 W stack based on 30 individual runs.

	MPA Model	PO Model
Min	0.5940	0.5940
Max	0.5940	9.9124
Mean	0.5940	1.4257
Median	0.5940	0.5941
SD	9.2137e-14	223.2178
RE	9.2137e-14	41.9981
MAE	1.8245e-15	0.8316
RMES	1.9452e-15	2.3469
Eff.	100.0000	83.6049
WILCOXON SIGNED RANK TEST		
P	1.6923e-06	1.7333e-06
Rank	1	1

PO optimization problem has the merits of the global solution (exploration) characteristics; this phase gives it the ability to reach the finest solution. However; its ability to locate the local solution (exploitation) is not very accurate based on its fifth phase. So, the PO algorithm can reach acceptable results with respect to those of the reported references as listed in table 3, 4, and 5.

Statistical analysis for both algorithms of MPA and PO have been performed. The results prove the robustness of the two algorithms with the superiority of the MPA algorithm as

proved from table 5, 6, and 7. Also, the same results can be investigated from figures 8, 10 and 14. It should be noted that the main reason is the good exploration and exploitation performance of the MPA.

VI. CONCLUSION AND FUTURE DIRECTIONS

A PEMFC is a nonlinear complicated dynamic system, which involves many interrelated parameters. This paper comprises the formulation of an optimization problem, which is devoted to optimal identification of the seven unknown parameters of the PEMFC. The MPA and PO optimization techniques have been utilized for solving the optimization problem, while the fitness function is presented by the sum of square errors (SSE) between the actual and estimated models. The proposed methods introduced the high performance with high matching degree respecting the measured data of different fuel cell stacks. The MPA and PO proved their effectiveness in reaching the optimal solution in a better way compared with the results in the literature. Moreover, the statistical tests have been performed to validate the robustness of the two algorithms. From the comparison, it is concluded that the MPA is an accurate method which can precisely extract the parameters of the PEMFC with different cases of study. Therefore, it is recommended that the MPA algorithm can be implemented for solving sophisticated highly integrated optimization problems. From a practical point of view, the estimated model can be used online with PEMFC for fault diagnosis and condition monitoring. Moreover, the estimated model also may be helpful in designing the real-time control PEMFC systems as well as system analysis. The future work, the analysis of the parameter's variations of the PEMFC model far from the standard operating conditions considering the presence of measuring noise should be studied. Furthermore, the application of other recent optimization algorithms such as Slime Mould Algorithm (SMA) and hybrid techniques to enhance the estimation process is one of the future directions. Additionally, more interest will be focused to enhance the performance of the PEMFC in the microgrid operation.

CONFLICTS OF INTEREST

The authors declare no conflict of interest.

REFERENCES

[1] H. A. Gaber, *Smart Energy Grid Engineering*, 1st ed. Amsterdam, The Netherlands: Elsevier, 2017, pp. 1–45. [Online]. Available: https://www.sciencedirect.com/book/9780128053430/smart-energy-grid-engineering

[2] International Atomic Energy Agency, Nuclear Energy Series No. NP-T-4.3 IAEA, Vienna, Austria. (2017). *Industrial Applications of Nuclear Energy*. [Online]. Available: https://www.iaea.org/publications/10979/industrial-applications-of-nuclear-energy

[3] A. L. Dicks and D. A. J. Rand, *Fuel Cell Systems Explained*, 3rd ed. Hoboken, NJ, USA: Wiley, 2018, pp. 69–133. [Online]. Available: https://onlinelibrary.wiley.com/doi/book/10.1002/9781118706992

[4] IEA, Paris, France. (2019). *World Energy Outlook*. [Online]. Available: https://www.iea.org/reports/world-energy-outlook-2019

[5] V. Quaschning, *Understanding Renewable Energy Systems*, 2nd ed. London, U.K.: Taylor & Francis, 2016, ch. 10.

[6] A. Arshad, H. M. Alib, A. Habib, M. A. Bashir, M. Jabbal, and Y. Yan, "Energy and exergy analysis of fuel cells: A review," *Thermal Sci. Eng. Prog.*, vol. 9, pp. 308–321, Mar. 2019.

[7] A. Sohani, S. Naderi, and F. Torabi, "Comprehensive comparative evaluation of different possible optimization scenarios for a polymer electrolyte membrane fuel cell," *Energy Convers. Manage.*, vol. 191, pp. 247–260, Jul. 2019.

[8] J. Cheng and G. Zhang, "Parameter fitting of PEMFC models based on adaptive differential evolution," *Electr. Power Energy Syst.*, vol. 62, pp. 189–198, Nov. 2014.

[9] Z. Sun, N. Wang, Y. Bi, and D. Srinivasan, "Parameter identification of PEMFC model based on hybrid adaptive differential evolution algorithm," *Energy*, vol. 90, pp. 1334–1341, Oct. 2015.

[10] A. Askarzadeh and A. Rezazadeh, "A grouping-based global harmony search algorithm for modeling of proton exchange membrane fuel cell," *Int. J. Hydrogen Energy*, vol. 36, no. 8, pp. 5047–5053, Apr. 2011.

[11] K. Priya, T. Sudhakar Babu, K. Balasubramanian, K. Sathish Kumar, and N. Rajasekar, "A novel approach for fuel cell parameter estimation using simple genetic algorithm," *Sustain. Energy Technol. Assessments*, vol. 12, pp. 46–52, Dec. 2015.

[12] Z.-J. Mo, X.-J. Zhu, L.-Y. Wei, and G.-Y. Cao, "Parameter optimization for a PEMFC model with a hybrid genetic algorithm," *Int. J. Energy Res.*, vol. 30, no. 8, pp. 585–597, Jun. 2006, doi: 10.1002/er.1170.

[13] L. Zhang and N. Wang, "An adaptive RNA genetic algorithm for modeling of proton exchange membrane fuel cells," *Int. J. Hydrogen Energy*, vol. 38, no. 1, pp. 219–228, Jan. 2013.

[14] O. E. Turgut and M. T. Coban, "Optimal proton exchange membrane fuel cell modelling based on hybrid teaching learning based optimization–differential evolution algorithm," *Ain Shams Eng. J.*, vol. 7, no. 1, pp. 347–360, Mar. 2016.

[15] M. Ali, M. A. El-Hameed, and M. A. Farahat, "Effective parameters' identification for polymer electrolyte membrane fuel cell models using grey wolf optimizer," *Renew. Energy*, vol. 111, pp. 455–462, Oct. 2017.

[16] A. A. El-Fergany, "Electrical characterisation of proton exchange membrane fuel cells stack using grasshopper optimiser," *IET Renew. Power Gener.*, vol. 12, no. 1, pp. 9–17, Jan. 2018.

[17] A. A. El-Fergany, "Extracting optimal parameters of PEM fuel cells using salp swarm optimizer," *Renew. Energy*, vol. 119, pp. 641–648, Apr. 2018.

[18] Y. Rao, Z. Shao, A. H. Ahangarnejad, E. Gholamalizadeh, and B. Sobhani, "Shark smell optimizer applied to identify the optimal parameters of the proton exchange membrane fuel cell model," *Energy Convers. Manage.*, vol. 182, pp. 1–8, Feb. 2019.

[19] S. Xu, Y. Wang, and Z. Wang, "Parameter estimation of proton exchange membrane fuel cells using eagle strategy based on JAYA algorithm and nelder-mead simplex method," *Energy*, vol. 173, pp. 457–467, Apr. 2019, doi: 10.1016/j.energy.2019.02.106.

[20] Y. Chen and N. Wang, "Cuckoo search algorithm with explosion operator for modeling proton exchange membrane fuel cells," *Int. J. Hydrogen Energy*, vol. 44, no. 5, pp. 3075–3087, Jan. 2019, doi: 10.1016/j.ijhydene.2018.11.140.

[21] A. Fathy, M. A. Elaziz, and A. G. Alharbi, "A novel approach based on hybrid vortex search algorithm and differential evolution for identifying the optimal parameters of PEM fuel cell," *Renew. Energy*, vol. 146, pp. 1833–1845, Feb. 2020.

[22] A. S. Menesy, H. M. Sultan, A. Korashy, F. A. Banakhr, M. G. Ashmawy, and S. Kamel, "Effective parameter extraction of different polymer electrolyte membrane fuel cell stack models using a modified artificial ecosystem optimization algorithm," *IEEE Access*, vol. 8, pp. 31892–31909, 2020.

[23] D. Miao, W. Chen, W. Zhao, and T. Demsas, "Parameter estimation of PEM fuel cells employing the hybrid grey wolf optimization method," *Energy*, vol. 193, Feb. 2020, Art. no. 116616.

[24] A. Faramarzi, M. Heidarinejad, S. Mirjalili, and A. H. Gandomi, "Marine predators algorithm: A nature-inspired Metaheuristic," *Expert Syst. Appl.*, vol. 152, Aug. 2020, Art. no. 113377.

[25] Q. Askari, I. Younas, and M. Saeed, "Political optimizer: A novel socio-inspired meta-heuristic for global optimization," *Knowl.-Based Syst.*, vol. 195, May 2020, Art. no. 105709, doi: 10.1016/j.knosys.2020.105709.

[26] H. H. EL-Tamaly, H. M. Sultan, and M. Azzam, "Control and operation of a solid oxide fuel-cell power plant in an isolated system," in *Proc. 9th Int. Conf. ICEENG*, vol. 9, 2017, pp. 1–13, doi: 10.21608/ICEENG.2014.30484.

[27] J. C. Amphlett, R. M. Baumert, R. F. Mann, B. A. Peppley, P. R. Roberge, and T. J. Harris, "Performance modeling of the Ballard mark IV solid polymer electrolyte fuel cell: II. Empirical model development," *J. Electrochem. Soc.*, vol. 142, no. 1, pp. 9–15, Dec. 2019.

[28] R. F. Mann, J. C. Amphlett, M. A. I. Hooper, H. M. Jensen, B. A. Peppley, and P. R. Roberge, "Development and application of a generalized steady-state electrochemical model for a PEM fuel cell," *J. Power Sources*, vol. 86, pp. 173–180, Mar. 2000.

[29] N. H. Saad, A. A. El-Sattar, and A. M. Mansour, "Adaptive neural controller for maximum power point tracking of ten parameter fuel cell model," *J. Electr. Eng.*, vol. 13, no. 3, pp. 233–239, 2013.
[30] M. Abdel-Basset, R. Mohamed, M. Elhoseny, R. K. Chakrabortty, and M. Ryan, "A hybrid COVID-19 detection model using an improved marine predators algorithm and a ranking-based diversity reduction strategy," *IEEE Access*, vol. 8, pp. 79521–79540, 2020, doi: 10.1109/ACCESS.2020.2990893.
[31] A. S. Menesy, H. M. Sultan, A. Selim, M. G. Ashmawy, and S. Kamel, "Developing and applying chaotic Harris Hawks optimization technique for extracting parameters of several proton exchange membrane fuel cell stacks," *IEEE Access*, vol. 8, pp. 1146–1159, 2020, doi: 10.1109/ACCESS.2019.2961811.
[32] A. Abbasi, B. Firouzi, and P. Sendur, "On the application of Harris Hawks optimization (HHO) algorithm to the design of microchannel heat sinks," *Eng. Comput.*, pp. 1–20, Dec. 2019, doi: 10.1007/s00366-019-00892-0.
[33] H. Chen, S. Jiao, M. Wang, A. A. Heidari, and X. Zhao, "Parameters identification of photovoltaic cells and modules using diversification-enriched Harris Hawks optimization with chaotic drifts," *J. Cleaner Prod.*, vol. 244, Jan. 2020, Art. no. 118778.
[34] Y. Song, X. Tan, and S. Mizzi, "Optimal parameter extraction of the proton exchange membrane fuel cells based on a new Harris Hawks optimization algorithm," *Energy Sour. A, Recovery, Utilization, Environ. Effects*, 2020, doi: 10.1080/15567036.2020.1769230.

AHMED A. ZAKI DIAB (Graduate Student Member, IEEE) received the B.Sc. and M.Sc. degrees in electrical engineering from Minia University, Egypt, in 2006 and 2009, respectively, and the Ph.D. degree from the Electric Drives and Industry Automation Department, Faculty of Mechatronics and Automation, Novosibirsk State Technical University, Novosibirsk, Russia, in 2015. Since 2007, he has been with the Department of Electrical Engineering, Faculty of Engineering, Minia University, as a Teaching Assistant and a Lecturer Assistant, where he was also an Assistant Professor with the Faculty of Engineering from 2015 to 2020. He held a Postdoctoral Fellowship position with the National Research University Moscow Power Engineering Institute (MPEI), Moscow, Russia, from September 2017 to March 2018. He was a Visitor Researcher (Postdoctoral) with the Green Power Electronics Circuits Laboratory, Kyushu University, Japan. Since 2020, he has been an Associate Professor with the Department of Electrical Engineering, Faculty of Engineering, Minia University. His current research interests include renewable energy systems, power electronics, and machines drives. He received the MIF Research Fellowship, Japan, in 2019.

MOHAMED A. TOLBA (Member, IEEE) received the B.Sc. and M.Sc. degrees in electric power and machines engineering from the Faculty of Engineering, Minia University, Minia, Egypt, in 2008 and 2013, respectively, and the Ph.D. degree from the Electric Power Systems Department, Moscow Power Engineering Institute (MPEI), National Research University, Moscow, Russia, in 2019. Since 2019, he has been an Assistant Professor with the Nuclear Research Center, Reactors Engineering Department, Egyptian Atomic Energy Authority, Cairo, Egypt. He is currently an Assistant Professor (Visitor) with the Electric Power Systems Department, MPEI, National Research University. He has more than 25 scientific research articles and papers that are published in high-impacted journals and conferences. His main research interests include power quality management, loss of electrical energy, optimization techniques/soft computing applications in electric power networks, renewable distributed sources, control systems, and operation management of distribution networks. He is a member of the IEEE IAS. He serves as the Co-Chair and the Technical Program Chair for the IEEE REEPE Conference, Moscow.

AYAT GAMAL ABO EL-MAGD received the bachelor's, master's, and Ph.D. degrees in electrical engineering from the Faculty of Engineering, Minia University, Egypt. She was an Assistant Lecturer with the Electrical and Computer Department, El-Minia Higher Institute of Engineering and Technology, Egypt, where she is currently an Assistant Professor. Her research interests include power systems control and renewable energy systems.

MAGDY M. ZAKY received the B.Sc.Eng. degree in control systems and instrumentation engineering from Menoufia University, Egypt, in 1992, and the M.Sc.Eng. and Ph.D. degrees in electrical power engineering from Cairo University, Egypt, in 2004 and 2013, respectively. Since 2015, he has been a Manager with the Egypt Second Research Reactor (ETRR-2), Egyptian Atomic Energy Authority (EAEA), where he has been an Associate Professor with the Engineering Department since 2019. He is the author of more than 30 articles. His research interests include control systems engineering, instrumentation, electrical power engineering, optimization, nuclear engineering, fiber grating and its applications, nuclear reactors safety analysis, energy management, project management, artificial intelligent, design of physical security systems, and fire systems.

ALI M. EL-RIFAIE (Senior Member, IEEE) received the B.Sc. degree in electrical power and machines, the M.Sc. degree in electrical power system engineering, and the Ph.D. degree in power system protection from Helwan University, Egypt, in 1998, 2005, and 2011, respectively. From 2000 to 2004, he was a Demonstrator with the Electrical Power and Machines Department, Faculty of Engineering and Technology, Helwan University. From 2005 to 2010, he was a Research Assistant with the Egyptian National Institute for Standards (NIS), where he was a Researcher with the High Voltage Metrology Laboratory from 2010 to 2015. He was also a Proficiency Test Manager and held a Laboratory Technical position. Since September 2015, he has been with the American University of the Middle East, Kuwait. He is currently an Associate Professor with the Electrical Engineering Department. He is the author of one book and several peer-reviewed conferences and journal articles in power system protection, electrical metrology, smart grids, and renewable energy. He is an active member in several peer-reviewed journals and conferences technical committees. He received twice the Best Paper from EEEIC, London.